The behaviour of potassium and sodium species during the thermal treatment of a demineralized Highveld coal

Lucinda Klopper

2011

Dissertation submitted for the degree Magister in Chemistry at the Potchefstroom Campus of the North-West University

Supervisor: Prof C.A. Strydom
Co-Supervisor: Prof J.R. Bunt

Declaration

I, Lucinda Klopper, hereby declare that the dissertation entitled:

The behaviour of potassium and sodium species during the thermal treatment of a demineralized Highveld coal

which I herewith submit to the North-West University in fulfillment of the requirements for the degree, MSc in Chemistry, is my own original work, and has not been previously submitted to any other educational institution. Recognition is given to all sources.

Abstract

A series of experiments was conducted to investigate the potential influence of pre- and post adding of catalysts to a demineralized coal char. The catalysts were chosen according to yield better catalytic activity and be inexpensive. CO_2 gasification was conducted on the samples in a temperature range of 500 °C to 900 °C. The coal chosen was a high-inertinite, high-ash, Highveld bituminous coal. The catalysts chosen were sodium carbonate, potassium carbonate, and a mixture of the two catalysts. Different methods were used to investigate the factors influencing the reactivity of the demineralized coal char, and the extent of the influence from the catalysts. Proximate analysis, ultimate analysis and ash yields were conducted on the starting material to determine the change the demineralization had on the coal. Ash fusion temperatures of the samples were also obtained. The results indicated that demineralization lowered the ash content, as well as the ash fusion temperatures, but the ultimate analysis showed consistency in both sets of samples. Mass losses obtained during the thermal treatment experiments under CO_2 atmosphere showed an increase in mass loss in the order of samples without addition of catalysts to the smallest amount of addition. Potassium carbonate showed the largest increase in mass loss during CO_2 thermal treatment, together with the mixture of the two catalysts. Samples with pre-added catalysts also had a larger mass loss than samples with post-added catalysts. According to the XRD and QEMSCAN results, some potassium species are retained in the ash, which is confirmed by XRF results. The XRF results also showed that the amount of alkali species retained is quite large.

Demineralized, Gasification, Catalyst, Potassium, Sodium

Opsomming

’n Reeks eksperimente is uitgevoer om te bepaal wat die potensiële invloed van voor- en later- toegevoegde kataliste op ’n gedemineraliseerde steenkool sintel sal wees. Die kataliste is gekies na aanleiding van beter katalitiese aktiwiteit, sowel as die feit dat hulle goedkoop is. CO_2 vergassing was uitgevoer op die monsters in die temperatuur gebied van 500 °C tot 900 °C. Die gekose steenkool is ’n hoë-inertiniet, hoë-as, bitumineuse Hoëveld steenkool. Die gekose kataliste was natriumkarbonaat, kaliumkarbonaat en ’n mengsel van die twee kataliste. Verskeie metodes was toegepas om die faktore wat die reaktiwiteit van die gedemineraliseerde steenkool sintel beïnvloed na te vors, asook die mate van invloed wat die kataliste bygedra het te bepaal. Aanvanklike analise, elementêre analise en as inhoud bepaling was uitgevoer op die begin materiaal om te bepaal watter moontlike veranderinge die demineralisering veroorsaak het in die samestelling van die steenkool. As fusie temperature van die monsters was ook bepaal. Die resultate het getoon dat demineralisering die as inhoud sowel as die as fusie temperature verlaag het, maar die elementêre analise het byna dieselfde resultate gelewer vir albei monsters. Massa verliese bepaal tydens die termiese behandeling eksperimente van die steenkool sintel onder CO_2 atmosfeer, het ‘n toename getoon vanaf die monster met geen katalis byvoeging tot die kleinste hoeveelheid katalis bygevoeg. Monsters met kaliumkarbonaat het die grootste toename in massa verlies getoon saam met die mengsel van die kataliste. Monsters met vooraf-toegevoegde kataliste het ook ’n groter massa verlies getoon as monsters met die katalis later toegevoeg. Na aanleiding van XRD en QEMSCAN analises blyk dit dat die daar kalium spesies in die as agter bly, wat ook bevestig is deur XRF resultate van die monsters. Die XRF resultate toon ook dat die hoeveelheid spesies wat agterbly ’n redelike groot fraksie is.

Gedemineraliseerde, Vergassing, Katalis, Kalium, Natrium

Acknowledgements

I would like to thank Prof Strydom, Prof Bunt and Prof Schobert for their dedication and hard work in helping me to complete this study. I would also like to thank SASOL for their financial and moral support during this study.

Table of Contents

List of Figures

List of Tables

Nomenclature

AFT	=	Ash fusion temperature
ASTM	=	American society for testing of materials
BET	=	Brunauer, Emmett and Teller isotherm
DAF	=	Dry ash free
EDXRF	=	Energy dispersive X-ray fluorescence
EPMA	=	Electron probe microanalyzer
FT	=	Flow/fluid temperature
FT-IR	=	Fourier transform infrared
HT	=	Hemispherical temperature
IDT	=	Initial deformation temperature
ISO	=	International standards organization
PDC	=	Partly devolatilized coal
SABS	=	South African Bureau of Standards
SANAS	=	South African National Standards
SEM	=	Scanning electron microscopy
ST	=	Spherical temperature
QEMSCAN	=	Quantitative evaluation of minerals by scanning electron microscopy
XRD	=	X-ray diffraction
XRF	=	X-ray fluorescence

Chapter 1

Problem Statement and Hypothesis

1.1 Problem Statement and Substantiation

Coal is a heterogeneous substance consisting of microscopically discernible, physically distinct, and chemically different components (macerals) along with inorganic components (mineral matter) mixed in varied proportions [Choudhury et al., 2004]. Potassium and sodium species regularly occur in coal but in different amounts and speciation within the mineral matter [Punjak et al., 1989]. Potassium mostly occurs in clay forms and sodium is present in clay as well. Alkali metals may also be bound in organic structures [Witthohn et al., 1998].

Thermal treatment of the coal releases potassium and sodium species in various forms. During the combustion process potassium and sodium volatilize in a similar chemical way, (due to their similar chemical characteristics), and at approximately the same rate [Witthohn et al., 1998]. They do not volatilize in the salt form, but reactions between halogen ions and the alkali metals occur in the gas phase above 500 °C. Above 1100 °C, potassium and sodium species can volatilize in elemental form. During thermal treatment of coal, gaseous alkali metals are released in two stages. (1) Firstly during the combustion of the coal, and secondly, (2) the less volatile forms are released from the ash [Davidsson et al., 2002a; Witthohn et al., 1998]. The emission of alkali compounds from the ash residue starts around 500 °C and increases exponentially up to 950 °C [Olsson and Pettersson, 1998]. At typical thermal conversion and combustion temperatures, alkali and alkaline earth metals react with various minerals present in coal to form sulphates, chlorides, silicates, hydroxides, and other compounds that participate in the formation of slags and fouling deposits [Dayton et al., 1999]. In a study it was found that the volatilization behaviour of the flue gas alkali emissions from the initial alkali metal content in the coal has a strong dependence on the chlorine content of the coal [Gottwald et al., 2002].

The catalytic effects of various deliberately added or inherent inorganic impurities on the rates of the gasification reactions of carbonaceous materials have been known for a long period of time [McKee, 1983]. Alkali additives have been used to promote the reactions between steam and air with coal and charcoal. Active catalysts also appear to

participate in the gasification processes by undergoing chemical and/or electronic interactions with the carbonaceous substrate [McKee, 1983]. The influence of a catalyst is very short-lived and it is effective only while in contact with a particular substrate [Nishiyama, 1991]. In the work of Nishiyama [1991] it was found that burn-off was increased with the addition of an alkali metal catalyst to Blair Athol char. An increase in the burn-off for the Blair Athol demineralized char with added catalyst was also seen. It is not clear if the demineralization of the coal had the greater effect than the catalyzed char. The removal of these water soluble minerals may have an effect on the reactivity of the coal. Several different methods are available to remove alkali species from coal such as washing with water, grinding the coal and sieving and acid leaching. Washing of coal with water removes almost all of the alkali metals dissolved as salts in the pore water of the coal [Jenkins et al., 1996]. Very harsh chemical fractionation can remove mineral matter (extraneous minerals and some included minerals) to yield a coal sample with less than 2% ash content/yield [Van Niekerk et al., 2008]. Organically bound sulphur is not a mineral but its concentration is in included in the ash content. Apart from the effects due to ion exchange and the removal of inorganics, it appears that hydrochloric acid/hydrofluoric acid demineralization has little, if any, effect on the macromolecular structure of coals [Larsen et al., 1989].

Gasification is a process that is gaining even more significance because it may be a possible route for saving more energy during coal conversion [Nishiyama, 1991]. Catalytic active compounds significantly increase the gasification rate of coal char at a given temperature. Examples used for catalytic gasification are: Pittsburgh No. 8, Blair Athol char, graphite, wood and an unnamed coal used by McKee [1983]. It may also lower the temperature of gasification, thereby attaining an advantage in product composition, and thus saving energy [Audley, 1987; McKee, 1983; Nishiyama, 1991]. The reactivity of carbonaceous materials such as graphite and coal char towards CO_2 and steam is strongly enhanced by the presence of alkali metal salts [Sheth et al., 2003]. Salts of the alkali and alkaline earth metals, as well as transition metals in the eighth group are active catalysts for gasification [Nishiyama, 1991]. Alkali and transition metals typically lower activation energies by several kilojoules per mole [Spiro et al., 1983b]. For these catalysts to function effectively in char gasification, a three-phase interface must be obtained between the carbonaceous substrate, the catalyst phase and the gaseous oxidant [Sheth et al., 2003; Silva and Lobo, 1986].

Bituminous coals are swelling coals and when they are soaked in an organic solvent they swell and form a gel [Cody et al., 1993]. If it is accepted that the physical structure of bituminous coals is a branched and highly entangled network, then the viscosity is directly related to the mobility of individual molecules within a swollen gel [Cody et al., 1993]. When bituminous coals are heated in the absence of oxygen they soften (352-452 °C) and become plastic. These thermoplastic properties can be reduced by addition of certain inorganic compounds such as alkali metal salts, to the coal before charring [Tromp et al., 1986]. The use of a catalyst to accelerate the steam gasification of coal is highly attractive, since it offers the possibilities of operating gasifiers at higher coal throughputs and lower temperatures [Veraa and Bell, 1978]. Char gasification is known to be the rate-determining step during coal gasification. The addition of alkali metal salts increases this rate-determining step [Sheth et al., 2003].

When looking at the mechanism of the interaction between alkali metals and char during CO_2 gasification, there are three phases that take part in the reaction [Silva and Lobo, 1986]. Considering a catalyst particle on a carbon surface, several different situations can be envisaged, but it is considered that the likely mechanism involves a normal gas/surface catalytic process at the exposed catalyst surface [Silva and Lobo, 1986]. The three phases are: (1) a gas phase, consisting mainly of CO_2; (2) a solid phase carbon which is the second reactant, and (3) a third phase (liquid or solid) operating in between as a catalyst [Silva and Lobo, 1986].

1.2 Hypothesis

Addition of different amounts of potassium carbonate, sodium carbonate and a mixture of the two may have a contributing or inhibiting effect on the CO_2 reactivity of a South African, inertinite-rich, demineralized bituminous coal char. The addition may also have an increasing effect on the total CO_2 conversion of the coal and coal char. The species of potassium present in the ash after CO_2 gasification may be in a recyclable form, such as free potassium oxide, chloride or chloride present in ash can be recycled. But potassium feldspars, illite and muscovite cannot be recycled.

1.3 Aims and Objectives

Aims and objectives of this study include:

- Demineralizing coal to remove the effect of the some mineral matter (inherent minerals, non-minerals and extraneous minerals) in coal for reactivity measurements and analytical experiments.
- Develop a method to determine relative CO_2 reactivity.
- Adding different amounts of catalyst and a mixture of catalysts before and after charring to determine the effects they have on CO_2 reactivity of the coal char.
- Focus on the influence of potassium and sodium carbonate additions (as well as a mixture of the two) to evaluate the catalytic effect of the formed potassium and sodium species.
- Using different analytical techniques to determine the forms of potassium and sodium species after thermal treatments and addition before and after charring.
- Determining the optimum amount of catalyst addition.
- Evaluating if there is a difference in adding the potassium and sodium carbonate before or after charring of the coal.
- To determine which species of potassium and sodium remain in the ash after CO_2 reaction.

1.4 Outline of Study

Figure 1.1 is a diagram representing the outline of the study. The experimental procedures followed were chosen according to the requirements of the outcomes of the study. The temperature range in which the experiments were performed was from 500 °C to 900 °C. The demineralization was done to eliminate influences of some mineral matter. The demineralization can remove both inherent minerals and organically bound inorganic elements. The coal was divided into two sets of samples i.e., (1) catalysts were added to coal before charring, and (2) catalysts were added to the coal (thus after charring) char. These samples were heated in a muffle furnace up to 900 °C under a CO_2 atmosphere. The mass loss after each run was measured. Ash fusion temperature (AFT), proximate analysis, ultimate analysis, X-ray fluorescence (XRF), X-ray diffraction (XRD) and QEMSCAN were performed to characterize the samples.

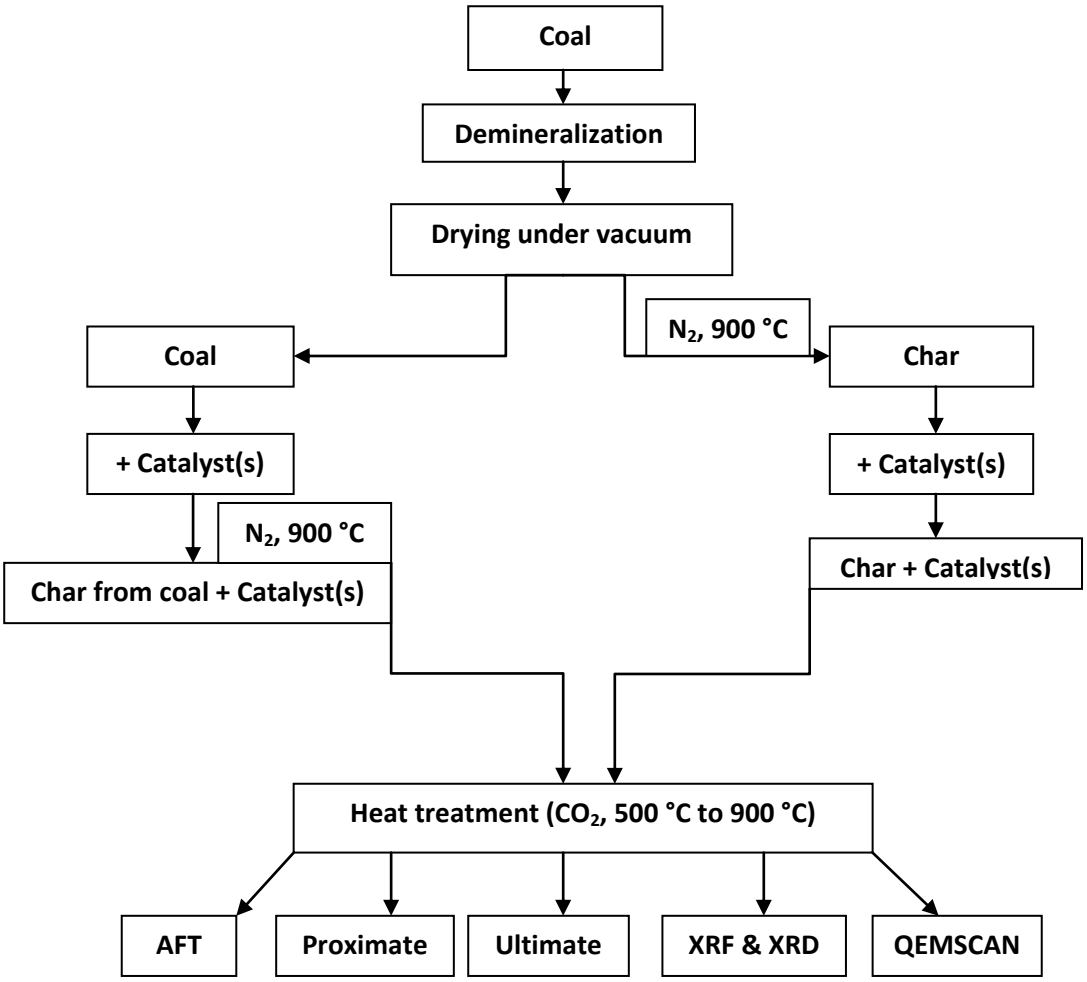

Figure 1.1: Outline of study

Chapter 2

Literature Review

2.1 Introduction

Coal from South Africa was found to have formed about 200 million years ago, which places South African coal in the Permian Gondwana Age [Cairncross, 2001; TSACPS, 2002]. Coal is the main energy source in South Africa and provides 79% of the country's total energy needs. However, using South African coal can be problematic, as it has a relatively high ash content (up to 30%) [Van Niekerk et al., 2008]. Mineral matter in coal is one of the biggest contributors to problems in coal combustion and gasification, including: fouling, slagging, corrosion, etc. [Barosso et al., 2006; Li et al., 2005]. Some of this inherent mineral matter may possibly also have a catalytic effect on the thermal conversion processes of coal [McKee, 1983].

Coal consists of two large fractions including: (1) mineral matter, which is mostly the inorganic species present in the coal and (2) macerals, which are the organic fraction of coal. The inorganic fraction in South African coal consists of about 125 minerals [Schobert, 2008]. The macerals can be divided into three main groups: (1) vitrinite, (2) exinite or liptinite, and (3) inertinite. Macerals are the organic components that constitute coal [Nip and De Leeuw, 1992]. The biggest difference between the Southern hemisphere Permian Gondwana coal and Northern hemisphere Carboniferous coal is the high inertinite content of some Gondwana coals, including Highveld coal [Van Niekerk et al., 2008].

The term inertinite was chosen to describe the infusible nature of certain highly reflecting macerals during carbonization [Bend, 1992]. Inertinite is a carbon-rich maceral group, and includes: micrinite, sclerotinite, fusinite, and semifusinite [Bend, 1992; Harrison, 1959]. Inertinite is usually finely divided and mixed in with vitrinite [TSACPS, 2002]. All inertinite macerals have a higher reflectance than the vitrinites, although differences diminish with increasing rank, and all inertinites have a higher carbon content than both vitrinite and liptinite [Bend, 1992]. Inertinite has no coking properties, and if it is in a high enough concentration, nullifies the coking properties of vitrinite [TSACPS, 2002].

The inertinite content formation may be attributed to the combined effects of weathering, the ablation of plant debris during the peat-forming stage, seasoned rainfall,

and a fluctuating water-table within a cool-temperate climate [Bend, 1992]. The formation of inertinite and semifusinite within Permian coal are mainly due to in-situ degradation and oxidation of the peat surface rather than the erosion, transportation and re-deposition of peat [Bend, 1992]. Peat is the first stage of six stages during the formation of coal. The six stages are: (1) peat, (2) lignite (brown and soft), (3) sub-bituminous (soft, crumbly, dull, dark brown/black to bright, jet black, hard and strong), (4) bituminous (dense, soft, black to dark brown), (5) lean coal and (6) anthracite (hard, brittle and black). Peat has the lowest fixed carbon content and the carbon increases in the order to anthracite with the highest fixed carbon content [TSACPS, 2002].

The focus in this review will be on the sub-bituminous and bituminous ranks, because the coal used in this research is an inertinite-rich bituminous Highveld coal. Highveld coal commonly ranges from sub-bituminous to mid-bituminous coals [Cairncross, 2001]. Sub-bituminous coal is a dull black coal, which is lower in moisture content and higher in heating value than lignite. On exposure to the natural elements, it tends to soften and crumble, and it does not cake together on heating [TSACPS, 2002]. The next stage in formation is bituminous coal, which is sub-divided into three categories namely: (1) low, (2) medium, and (3) high rank according to increasing age, depth of burial and geothermal temperature [TSACPS, 2002]. These two ranks have high sufficient heating value, as well as a high calorific value, to effectively use in the combustion processes. These values are important for further effective thermal treatment of the coal.

Coal is thermally processed to yield usable products. Coal gasification has emerged as a clean and effective way for the production of gaseous fuel and/or synthesis liquid fuel precursor [Zhu et al., 2008]. Gasification is a proven thermo-chemical process that converts hydrocarbons such as coal or liquids to a synthesis gas by means of partial oxidation with oxygen, CO_2 or steam [GTC, 2008; Probstein and Hicks, 2006; Schobert, 2008]. Although this term is generally reserved for processes involving chemical changes, evaporation by heating is also included [Probstein and Hicks, 2006]. It is a flexible, commercially proven, and efficient technology that produces the building blocks for a range of high-value products from a variety of low-value feedstocks [GTC, 2008; Schobert, 2008]. When a hydrocarbon feedstock is injected with oxygen and steam into a high-temperature pressurized (or non-pressurized) reactor until chemical bonds of the feedstock are broken, it is called gasification [GTC, 2008]. During gasification clean products are produced without the impurities of the parent coal, especially sulphur and ash [Schobert, 2008].

Gasification technologies represent a significant advancement and benefit over combustion or incineration technologies, due to its innate ability to control most pollutants and its ability to produce multiple products [Spiro et al., 1983a]. Gasification is mostly used to produce synthesis gas [GTC, 2008; Hutchinson, 2009; Probstein and Hicks, 2006]. During gasification the products are CO, H_2, N_2, H_2S and no oxygen, whereas during combustion the products are CO_2, H_2O, NO_x, SO_2 and oxygen [GTC, 2008]. The greatest difference between gasification and combustion is that the oxygen supply is limited during gasification, whereas there is an over-supply of oxygen during combustion [Hutchinson, 2009].

This chapter reviews the mineral matter in coal, with special focus on potassium and sodium species, and potassium and sodium as catalysts. Furthermore, a review is given of the thermal processes concerning coal and char; physical, chemical and structural aspects of coal and coal char, and the influence of alkali catalysts on reactivity of coal and char. Mechanisms for the catalyst-substrate interactions are also discussed.

2.2 Mineral Matter

Coal consists of organic matter (macerals) together with different types of inorganic constituents; the latter consisting of minerals, non-mineral inorganic elements and trace minerals [Matjie et al., 2008]. Mineral matter is the inert solid material in coal, and like moisture, it reduces the heating value of coal by dilution of the fixed carbon content. After thermal processing of the coal, the mineral matter remains in a slightly altered form as ash [TSACPS, 2002]. Mineral matter occurs in two possible forms in the coal: (1) inherent or included mineral matter and (2) extraneous or excluded mineral matter.

Inherent mineral matter is the mineral matter that is intimately mixed with the coal or closely associated with the organic matter or macerals in the coal [Liu et al., 2007; McLennan et al., 2000; TSACPS, 2002; Ward, 2002]. These macerals contain minerals present in the original vegetation from which the coal was formed, and finely divided clays and similar materials carried into the swamp by water or wind [TSACPS, 2002]. These clays are intimately mixed with the coal substance, and cannot be removed by coal beneficiation techniques. All South African coals contain varying quantities of such intimately mixed minerals. Such minerals would include finely dispersed clays, quartz, carbonate and pyrite group minerals [TSACPS, 2002].

Extraneous mineral matter dirt bands and lenses in the seam, shales, sandstones and intermediate rocks introduced into the mined product from the roof and floor of the seam. Most of this material is free and easily removed by coal beneficiation techniques. In some cases the impurities are strongly attached to the coal, but can be largely freed from the coal by finer crushing [TSACPS, 2002].

The non-mineral inorganic components typically include Ca, Mg, Na and other elements occurring as dissolved salts in the pore waters, as exchangeable ions attached to carboxylates and other functional groups; and metallic salts of carboxylic acids forming part of the macerals [Matjie et al., 2008]. These non-mineral inorganic material found in coal come into the coal in various ways. According to Schobert [2008] the main source is via the plant material which is present during the formation of the coal; the second source of minerals in coal is those that were deposited in the coal via the minerals deposited in the swamp during coalification. These minerals may be washed into the swamp because of erosion of rocks in the vicinity. The third possibility is the reaction of water molecules in the coal that was percolating through the coal during formation. Minerals in coal occur in one of five main modes: (1) as small granular inclusions (disseminated); (2) as lenses or layers (partings); (3) as concretions (nodules); (4) within cracks or cleats (fissures); (5) or as large masses of rocks (rock, fragments) [Bend, 1992].

Mineral matter (including alkali metals in coal) can be divided into three categories [Westberg et al., 2003]. The first category is where the inorganic species is associated with the organic species, mainly in the form of carboxylics. The second category includes the occurrence of the inherent minerals that were formed at the same time as the coal, and which are finely divided throughout the coal matrix in horizontal assemblages. Potassium is found as simple salts such as potassium hydroxide, potassium carbonate and potassium chloride. The third category is the occurrence of minerals formed by precipitation form various water solutions penetrating the coal layer, i.e. water containing dissolved salts being transported downward from the surface, or hydrothermal solutions rising in pores and cracks. These minerals are often located in vertical formations in the coal seam because of the perpendicular movement of the water. Alkali metals are mostly found dissolved in pore water as salts [Westberg et al., 2003]. Potassium found in category two is chemically very stable, because it is part of the inherent mineral constituents. The mineral matter has a catalytic effect which will differ according to its distribution in the carbonaceous matrix and coal rank [Adánez et al., 1985]. In some cases, potassium is also found as potassium

feldspars (Sanidine ($KAlSi_3O_8$)) and illite ($K_{1.5}Al_4(Si_{6.5}Al_{1.5})O_{20}(OH)_4$) in the coal [Gobrilsch et. al., 1984; Ward and French, 2004]. McKee et al. [1983] found that other mineral impurities can adversely affect the reactivity of the catalysts. Potassium carbonate, sodium carbonate and a 1:1 mixture of the two catalysts were used as catalysts in this study.

2.2.1 Inherent Potassium and Sodium Species in Coal

According to Schobert [2008], potassium carbonate and sodium carbonate species are two of the 125 minerals present in coal. Potassium mostly occurs in clay forms in the coal mineral matter. Sodium (predominantly as sodium chloride) is mostly present as a salt and to a lesser extent present in clay. Of the many alkali compounds released into the gas phase, the chloride forms (NaCl and KCl) have been identified as the major speciation of the alkali after the combustion or gasification of coal. Both potassium and sodium are present as chlorides, and to a lesser extent as hydroxides, in the gas phase in both modes of operation (i.e. combustion and gasification) [Mojtahedi and Backman, 1989]. This is attributed to alkali metals having a very high affinity to chlorine [Li et al., 2005]. Mojtahedi and Backman [1989] found that under combustion conditions both potassium and sodium seem to condense as sulphates (Na_2SO_4 and K_2SO_4). Under gasification conditions, chlorides and carbonates dominate in the condensed phase and this is supported by Punjak et al. [1989]. The volatilization of alkali metals shows strong dependence on the chlorine content of the feedstocks. Spiro et al. [1986] reported that potassium is a particularly pernicious impurity in coal and that potassium fluxes other normally refractory materials which lead to extensive deposits in combustors.

Potassium is found in illite, orthoclase, leucite, and sylvite according to analyses done by Spiro et al. [1986]. It was also found in muscovite and biotite. The dominant form of potassium is in the layered aluminosilicate structure exemplified by illite. Muscovite is a reasonable product of illite metamorphism in the absence of organic matter. Illite represents a class of abundant clay minerals. It has also been speculated that illite catalyses the formation of coal and illite is the most finely divided mineral species in coal [Spiro et al., 1986]. Potassium can occur in one of three possible ways: (1) potassium is bound to the surface of clays rather than inside the layered structure, (2) may be adsorbed on a wide range of surfaces including mineral and organic, and (3) it is possible that potassium is dissolved in water-filled pores [Spiro et al., 1986]. In peat, the potassium seems to exist in soluble form in much lower quantities, with the surface layers of peat showing the highest

soluble potassium concentrations. There is evidence that organically-bound inorganic elements in solid fuels such as peat are released more easily and at lower temperatures than if they were bound in compounds such as silicates [Mojtahedi and Backman, 1989].

Potassium forms low melting phases with iron and sulphate species [Spiro et al., 1986]. The fate of potassium during processing and utilization shows that only at very high temperatures (above 1000 °C) does illite undergo major reorganization. Spiro et al. [1986] proved with experimental results that illite just loses surface water during low temperature ashing. When illite is decomposed and completely melted the potassium-aluminosilicate compound will form a glass phase which causes problems with agglomeration during thermal processing of the coal [Spiro et al., 1986]. The volatile sodium species can react with silicates/aluminosilicates during its volatilization from coal, to form non-volatile composites. Potassium is evolved from aluminosilicates through a replacing reaction by volatilized sodium in flue gas, which means that the amount of released potassium is dependent on the sodium content in the coal [Zhang et al., 2001]. Weeber et al. [2000] found that the presence of kaolinite is positively correlated to higher ash fusion temperatures. Kaolinite refers to a group of clay minerals. Kaolinite is the most common mineral in kaolin. When kaolin is heated, water is released at temperatures of 400-600 °C, and an amorphous mixture of alumina and silica called meta-kaolinite is formed [Tran et al., 2003]. In coal, part of the alkali metal content is dispersed in the mineral phases, limiting the vaporization of alkali material [Olsson et al., 1997].

Sodium exhibits less interaction with the carbon than potassium, and as a consequence the carbonate is less easily or to a lesser extent dissociated and dispersed over the carbon, as inferred from in-situ FT-IR experiments performed by Kapteijn et al. [1986]. Potassium carbonate and sodium carbonate are used as catalysts and the catalytic effect of these metals are discussed in more detail.

2.2.2 Potassium and Sodium Species as Catalysts

The main role of a catalyst is to increase the steady state concentration of oxygen at the carbon surface by increasing the total number of active sites [Kapteijn et al., 1986]. Catalysis is assumed to be due to an increase in concentration of ion radicals at the surface [Moulijn et al., 1984]. Studies have shown that the most active catalysts in carbon gasification by steam and CO_2 are alkali metal salts such as alkali carbonates, oxides, hydroxides and chlorides [Lang, 1986; McKee et al., 1983; Moulijn et al., 1984; Nishiyama,

1991; Spiro et al., 1983b; Suzuki et al., 1992; Zhu et al., 2008]. The catalytic species are oxidic rather than metallic [Moulijn et al., 1984]. In the case of sodium the number of active sites seems to be temperature dependent due to carbonate formation and decomposition [Kapteijn et al., 1986]. There are two possible routes to release sodium during the coal utilization process, i.e. either as a NaCl or as atomic sodium [Zhang et al., 2001]. Among the alkali metals, potassium shows the best catalytic activity for all coal ranks [Kühn and Plogmann, 1983; Veraa and Bell, 1978] due to the formation and dispersion of a liquid-solid interface between potassium and the carbon surface [Zhu et al., 2008]. K_2CO_3 and KOH are found to be the most active potassium compounds. These two components appear to follow the same catalytic mechanism and show the same activity for equivalent amounts of potassium [Sams and Shadman, 1983].

Since the gasification reactions occur at the gas-solid interface, the available catalyzed surface area is of major importance [Hamilton et al., 1984]. The effect of loading method on the catalytic activity of potassium carbonate will be small [Liu and Zhu, 1986; Moulijn et al., 1984]. Thus, potassium carbonate has almost the same effect on reactivity for either impregnated coal or mechanically loaded coal [Liu and Zhu, 1986]. The efficacy of potassium is independent of coal rank, when the reactivity is measured with and without catalyst [Nishiyama, 1991; Takarada et al., 1986]. The physical properties of the fluid mass of bituminous coal is changed by the reaction of potassium carbonate, thereby increasing the available and accessible surface area of the char and enhancing the reactivity of the char [Tromp et al., 1986]. The primary contributing factors are the change in the reaction area and the change in the amount and distribution of catalyst during gasification [Hamilton et al., 1984].

It is suggested that the increase in area at low conversions is due to catalyst mobility and unplugging of pores [Hamilton et al., 1984]. Potassium ions are mobile catalysts when exposed to heat [Nishiyama, 1991; Wood et al., 1984]. Examination of samples treated by mechanically mixing potassium carbonate and impregnation of the catalyst showed that the char surface was very uniform when using either method [Liu and Zhu, 1986]. In a study conducted by Takarada et al. [1986] the potassium catalyst on char, ranging from anthracite to lignite, was found to be dispersed so uniformly that the catalyst particles were rarely observed with scanning electron microscopy. The carbonate salts of potassium and sodium have been found to decompose during heating and it is generally found that decomposition

occurs below the melting temperature of the salts [Moulijn et al., 1984; Suzuki et al., 1984]. Mobility of the catalyst is thus vitally important for its effectiveness.

Nishiyama [1991] reported that demineralization of coal noticeably enhances of activity noticeably for potassium. The number of catalytic sites, which are under the influence of the added catalyst, determines the reactivity of a catalytic system. The reactivity of coal char towards carbon dioxide and steam is known to be enhanced by the presence of alkali metal salts [McKee et al., 1983; Sheth et al., 2003]. Effective gasification catalysts are ionic salts, which can conduct an electrical current, particularly at elevated temperatures [Wood et al., 1984].

It was proposed that potassium carbonate decomposes and forms a surface intermediate, K-O-C, and thus potassium is atomically dispersed on the carbon surface [Takarada et al., 1986]. A non-stoichiometric oxide with excess of metal is formed leading to covalent M-C bonds. By this action the aromatic character would be decreased and, as a consequence, acceleration of the reaction occurs [Moulijn et al., 1984]. The melting temperatures of sodium carbonate and potassium carbonate are 851 °C and 891 °C, respectively [Suzuki et al., 1984]. Molten solutions of the catalysts are better able to penetrate the coal structure and through this way improve accessibility of the unavailable carbon sites in the interior of the coal/char [Sheth et al., 2003]. Studies with graphite [Sheth et al., 2003] have shown that oxidation rates rapidly increase at temperatures close to the melting temperatures of the catalysts. It was found that the gasification rates of coal char in CO_2 in the temperature range of 700 °C – 900 °C can be considerably increased by the addition of binary eutectic salt catalysts, because eutectic salts have lower melting points than the separate salts [Sheth et al., 2003]. An in-situ FT-IR experiment done by Suzuki et al. [1989] confirmed the presence of phenoxide-like structures in K_2CO_3 loaded char during CO_2 gasification at 500 °C. The catalytic oxidation involves two processes on two sites; i.e. one is the dispersing of the alkali metal, and the other is the formation of alkali metal clusters. The dispersed alkali metal is rapidly oxidized. The catalyst reduction involves to process corresponding to the two processes in the catalyst oxidation [Suzuki et al., 1992].

Results from experiments with Somerset C ash containing 12%, 25%, 43% and 67% added K_2CO_3, indicated that the addition of potassium carbonate lowers the ash fusion temperature of the ash up to a concentration of 10% K_2O present, but it increases again at higher K_2CO_3 concentrations [Huggins et al., 1981]. These results are shown in Figure 2.1 taken from Huggins et al. [1981].

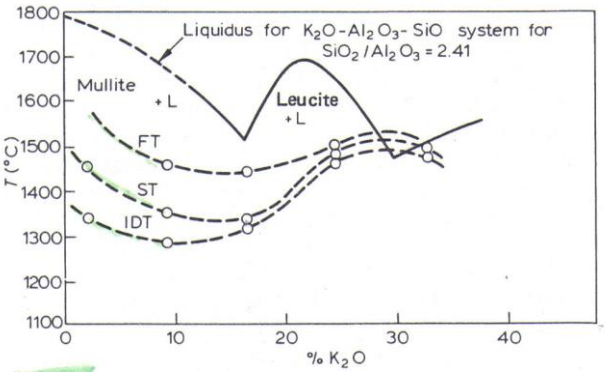

Figure 2.1: The effect of potassium carbonate on the ash fusion temperature of Somerset C ash. K_2CO_3 mixtures plotted against weight percent K_2O. [Taken from Huggins et al., 1981].

According to Schobert [2008] one of the complications of using alkali metals as catalysts are that they sinter at too high temperatures and particles melt and fuse together. This causes a reduction in total surface area of the catalyst and thus lowers the catalyst activity. There is unfortunately no method to unsinter a sintered catalyst. With increasing temperature (above 1000 °C), the catalytic effect of alkali metal salts was found to decrease when added to a Linnanchang coal char [Liu and Zhu, 1986]. The physical properties of coal and coal char also have a big effect on the reactivity, as discussed in the next section.

2.3 Physical Properties of Coal

The physical properties of coal from different sources and sometimes the same source, such as colour, specific gravity, and hardness, vary considerably. This variance depends on the composition and the nature of preservation of the original plant material that formed the coal, the amount of impurities in the coal, and the amount of time, heat and pressure that has affected the coal since it was first formed [Bend, 1992].

Interactions occurring at the coal char surfaces are heterogeneous and the accessibility of gaseous reactants as well as specific surface areas are very important. The accessibility to this surface area is dependent on the pore structure morphology of the char, for example the pore size distribution, tortuosity, intersections, shape etc. The porosity morphology of coal chars varies over a considerable range and is determined by a large number of factors including: (1) the nature of the porosity of the precursor material prior to coalification, (2) the coalification process, and (3) extent and method of any subsequent

activation or gasification [Adánez et al., 1985; Calo and Zhang, 1995]. Micropores can become more accessible to reactant gases from a loss of volatile matter. Micropores have a diameter < 2 nm [Dutta et al., 1977]. The proportion of micropores generally increase with rank and such pores are predominant at high rank, whereas macropores are predominant in low-rank coal [Clarkson and Bustin, 1996]. If the processing temperature is too high, microporosity in the char is rapidly lost. This is a result of thermal breakage of cross-links between planar regions in the char, allowing improved alignment of these regions with loss of porosity between regions [Walker and Hippo, 1975]. Clarkson and Bustin [1996] used a transmission electron microscope to determine the pore size and porosity distributions associated with the three major maceral groups (vitrinite, inertinite and liptinite). Vitrinite was found to be mainly micro- and mesoporous; inertinite (the most porous maceral group) was found to be mainly mesoporous; and liptinite, the least porous maceral group, was found to be mostly macroporous [Clarkson and Bustin, 1996]. Microporosity of coal decreases with an increase in total inertinite and mineral matter content [Clarkson and Bustin, 1996].

According to Schobert [2008] there are three pyrolysis stages prevalent during coal devolatilization. Stage one pyrolysis occurs at <200 °C and this is a slow reaction. During this stage the primary products are water, the oxides of carbon, and hydrogen sulphide. Stage two pyrolysis occurs at temperatures between 350-550 °C and these reactions are fairly fast. The main products are light gaseous hydrocarbons and a variety of condensable organic compounds leading to tar. This is the stage where char forms. Char is a solid that has not passed through an intermediate fluid phase. Third stage pyrolysis occurs at >550 °C and well above. The reactions are slow and a wide variety of small molecules are released.

During gasification or combustion of a bituminous coal it was found that the micropore structure is dramatically altered, while that of the macropores (> 50 nm) is only moderately affected [Tseng and Edgar, 1989]. As gasification was performed on a Wyodak coal char, micropores developed to the maximum in the surface area, and thereafter some of these micropores became mesopores (2-50 nm) (or even macropores); i.e., the population of micropores began to decrease. During this experiment Calo and Zhang [1995] found that loss of surface area occurred at high conversion. This was caused by a larger porosity that developed during which some of the pore walls collapsed as burn-off proceeded. In the research of Dutta et al. [1977] it was found that the char-CO_2 reaction developed new surfaces by enlarging the micropores of the solid to some extent, but principally by opening

up pore volumes not previously available to reactant gas. Unavailable pore volumes were attributed to the micro-capillaries that were too small or existing pores that were not connected. During the reaction, the surface area increased up to a point when the rate of formation of new areas were paralleled by the rate of destruction of the old areas. Surface area decreased on further conversion [Dutta et al., 1977]. The different rate characteristics of coals and chars were apparently due to the difference in their pore characteristics, which again change with conversion and temperatures.

The oxidation of the char surfaces mainly depends, among many other aspects, on the oxygen concentration in the gas and also on the amount of volatiles released by the pyrolyzing coal particles [Alvarez and Borrego, 2007]. As the cloud of volatiles surrounding the coal will be preferentially consumed by the oxygen, thus preventing the O_2 from reaching the solid surface during the pyrolysis stage [Alvarez and Borrego, 2007]. This is one of the main differences between gasification of coal and gasification of char. The gasification of char is a bit faster than for coal, in the initial devolatilization stages of coal as the char had already lost its volatiles.

2.4 Macromolecular Chemical Structure of Coal

Much of coal's chemistry can be determined by its macromolecular structure [Larsen et al., 1989]. The chemical behaviour of biopolymers present in plant material, upon coalification, determines the greater part of the chemical structure of a coal [Nip and De Leeuw, 1992]. Vitrinite, the main component of most types of bituminous coal, consists of a porous, cross-linked macromolecular network, where the cross-links can be due to covalent bonds, hydrogen bonds, or entanglements between the macromolecules [Larsen et al., 1989; Lucht et al., 1987; Ndaji et al., 1997; Schobert, 2008]. Non-covalent interactions such as hydrogen bonds and ππ-interactions are also important [Ndaji et al., 1997]. Micropores and ultra-micropores make out a large fraction of most ranks of coal [Walker, 1981]. Water is found in these pores, because coal has a high affinity for water molecules that are strongly held by the coal structure. The removal of the inherent moisture during sample pre-treatment can collapse the interconnected pore network [Amarasekera et al., 1995]. This is especially true for coals of lower rank. Lower rank coals have a larger fraction of macropores, compared to micropores, and can thus hold a larger volume of water. It was suggested that the network of pores with inherent moisture house a complex mixture of

dissolved molecules such as sodium chloride and potassium chloride [Larsen et al., 1989; Ndaji et al., 1997].

A model was constructed using high volatile bituminous coal illustrating some of the chemical structure of the coal [Hill and Lyon, 1962]. The model can be used to predict possible pyrolysis products from thermal degradation [Veras et al., 2002]. Bituminous coals have a branched and highly entangled network [Cody et al., 1993]. It was suggested that coal consists of large heterocyclic nuclei monomers (aromatic and hydro-aromatic layers), with alkyl side chains that is held together by three-dimensional C-C groups, terminated at their edges by various functional groups and cross-linked by various functional groups [Hill and Lyon, 1962; Walker, 1981; Walker and Hippo, 1975]. These groups include ether oxygen bonds, methylene groups and functional oxygen groups [Hill and Lyon, 1962; Lucht et al., 1987; Ndaji et al., 1997; Walker, 1981; Walker and Hippo, 1975]. The average size of these layers and the number aligned closely parallel increase with increasing rank of coal [Walker and Hippo, 1975]. The forces holding the large macromolecular molecules of the coal together are not known [Lucht et al., 1987]. More or less poor alignment between packets of layers produces internal porosity and results in coal being a microporous material [Walker and Hippo, 1975]. Oxygen is interchangeable with sulphur in some structures [Hill and Lyon, 1962]. Large condensed nuclei were said to have the same simple aliphatic side chains and nitrogen was observed to occur mainly in the heterocyclic ring structures [Hill and Lyon, 1962]. In many high volatile bituminous coals, it was seen that long-chain, simple aliphatic and alicyclic hydrocarbon groups predominated [Hill and Lyon, 1962].

The macerals that are derived from different plant materials consist of a number of different chemical compounds, which is explained by the fact that the plants consisted of a number of different chemical compounds [Nip and De Leeuw, 1992]. Upon thermal treatment all coals release volatile matter, primarily from the periphery of the layers. Some coals do not soften upon thermal treatment and are converted to a char. The micropore structure which was in the precursor coal is essentially preserved in the char if the char is not formed at a too high temperature [Walker and Hippo, 1975].

The macromolecular structure of coal is thus a complex structure of molecules, including alicyclic rings, oxygen molecules, nitrogen molecules, sulphur molecules, etc. Coal is also hygroscopic, and when these associated water molecules are removed the delicate intermolecular network of the coal can collapse. The unorganized structure of lower rank coal forms the microporosity of the coal. This in turn influences the gasification rate

(reactivity) of the coal/char. Gasification, as well as, catalytic gasification is discussed in more detail in the following section.

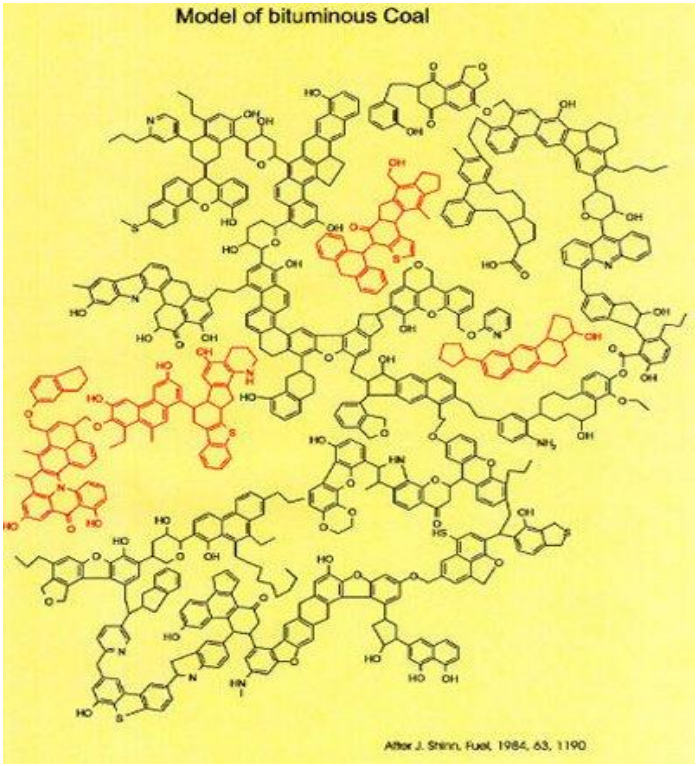

Figure 2.2: A model of bituminous coal [Shinn, 1984].

Figure 2.2 shows a possible model of bituminous coal as presented by Shinn [1984]. This shows the aromatic structure as well as the functional groups that coal can possibly terminate in. Due to the heterogeneity of coal, complex complete accurate models are the closest representation, even though it can never completely describe coal.

2.5 Gasification

As mentioned previously, gasification is the partial conversion process of carbon to synthesis gas via reaction with CO_2 or steam. Gasification is used as a clean technology that combines the economic advantages of coal with the environmental benefits of natural gas [Hutchinson, 2009]. Modern gasification technologies adapted will generally operate as follows [adapted from Hutchinson, 2009]:

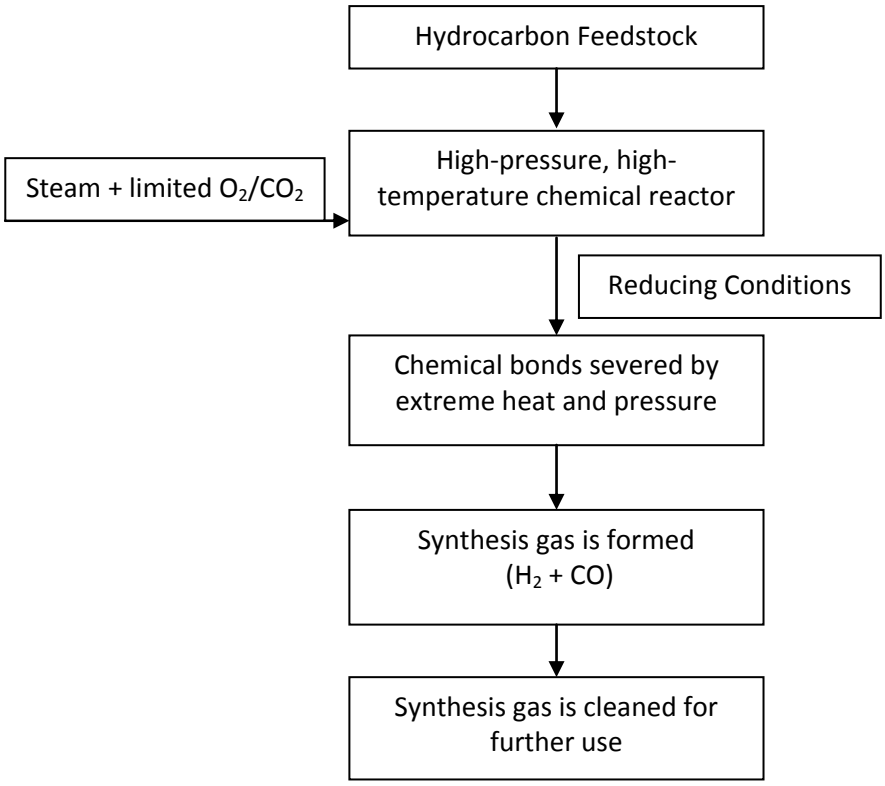

Figure 2.3: A schematic representation of a modern gasification process adapted from Hutchinson [2009].

In Figure 2.3 a general gasification process is described, giving a rough outline of the process operation. A hydrocarbon feedstock (often low quality) is fed into a high-pressure, high-temperature chemical reactor. In the reactor, steam and a limited oxygen flow are pumped in to interact with the feedstock. In the resultant reducing atmosphere the chemical bonds of the feedstock are broken by the severe heat and pressure conditions they experience. This severing of the bonds forms synthesis gas which consists mainly out of hydrogen and carbon monoxide. The formed synthesis gas is then cleaned for further use [Hutchinson, 2009].

The difference between gasification and combustion is the oxygen availability between the two processes. Combustion (or burning) is an exothermic reaction between a fuel and an oxidizer, whereas gasification is an exothermic reaction between a carbonaceous fuel and an oxidizer in a reactor where the oxygen supply is limited from 20% to 70% of the oxygen necessary for complete combustion [Hutchinson, 2009].

There are three categories of gasifiers which depend on the feedstock in the gasifier: i.e. (1) moving-bed, (2) entrained flow and (3) fluidized-bed. Moving bed gasifier is where the carbonaceous fuel is dry-fed through the top of the reactor. It reacts with the gasifying agents while moving in a counter-current of co-current through the bed with any net solids flow [Hutchinson, 2009; Probstein and Hicks, 2006]. As a result the bed moves downward. This is a continuous process and the remaining ash is dry. During entrained flow there is no longer a distinct bed [Hutchinson, 2009; Probstein and Hicks, 2006]. The feedstock may be dry-fed or slurry and goes through the various stages of thermal conversion as it moves with the gasifying agent flow. The synthesis gas leaves at the top of the reactor and the ashes flow out the bottom as a slag. The gasifier need not be vertically orientated, just as long as the gas or liquid flow maintains the solids in an entrained or slurried state. The operating temperatures are very high. In the fluidized-bed category the fuel is introduced into an upward flow of gasifying agent, during which it remains suspended in the gasifying agents while the thermal conversion process takes place. The particle size tends to be smaller compared to particle sizes used in other gasifiers. The temperature at which this takes place is much lower, thus the ashes can be removed in the dry form [Hutchinson, 2009]. A gasification reactor can be divided into four zones: (1) drying zone, (2) devolatilization zone, (3) reduction zone, and (4) combustion zone. The zones are distinguishable in a fixed-bed gasifier as shown below in Figure 2.4 [Hebden and Stroud, 1981].

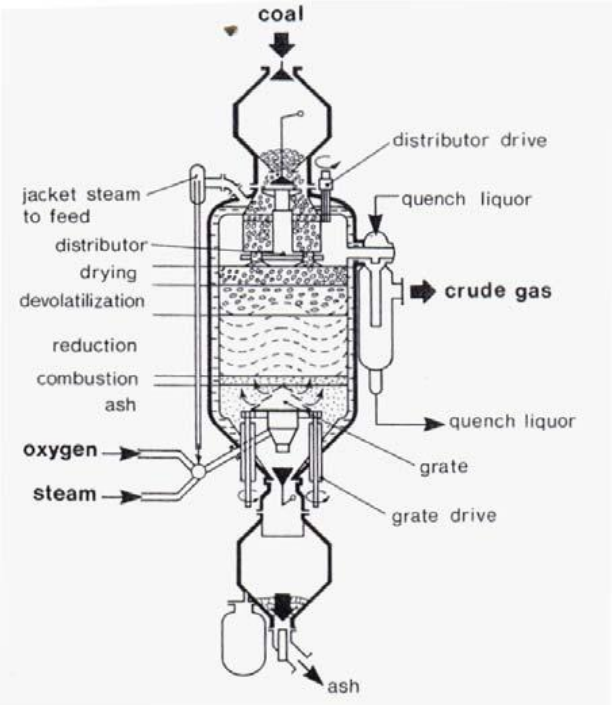

Figure 2.4: Schematic of a fixed-bed gasifier. [Hebden and Stroud, 1981]

The different zones can be observed in Figure 2.4. The first is the drying zone is at the top, followed by the devolatilization and reduction zones respectively. The combustion zone can be found near the bottom between the reduction zone and ash-bed [Alvarez and Borrego, 2007]. The different zones can also be seen more clearly in figure 2.5.

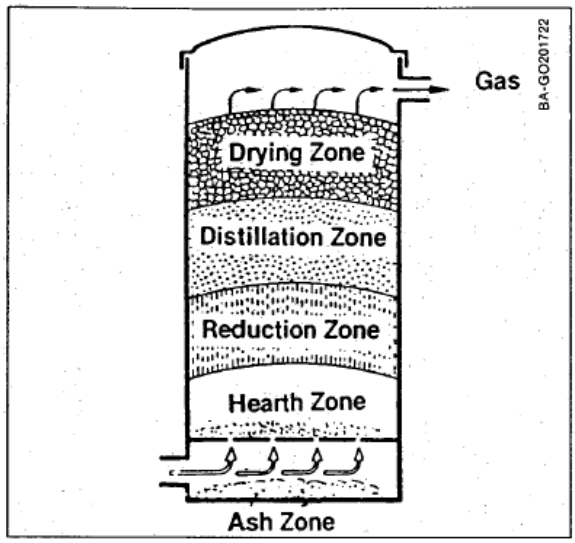

Figure 2.5: Simplified schematic illustrating the different zones.

Gasification is used in most of the world such as Africa, Asia, Europe, Australia and North America to convert coal into more useful products. Schobert [2008] reported that carbon does not gasify evenly, i.e. some sites on the carbon matrix gasify more readily than others. These sites that are particularly active are known as active sites. The activity of a catalytic system is determined primarily by the number of active sites which are under the influence of the catalyst. The surface area can be related to the number of active sites in cases where the amount of catalyst is sufficient to cover available surface area at the time of loading [Nishiyama, 1991]. These sites are often located at the edges of carbon layers and as a rule edge atoms are more reactive than basal plane atoms [Schobert, 2008]. Coals display various degrees of porosity where gaseous reagents are able to penetrate the pore system and react at interior surfaces [Schobert, 2008]. The characteristics of these pores may be very important in determining the overall reactivity and up to 90% of the total surface area can be internal pore surfaces [Schobert, 2008].

Gasification can be divided into two distinct stages: (1) the first stage is pyrolysis and (2) the second stage involve to char-CO_2 reactions. Pyrolysis usually starts at about 350-400 °C and is almost complete at about 1000 °C. Pyrolysis can be completed in seconds [Dutta et

al., 1977]. Reactivity in the first stage is mainly a function of the mineral matter of the char/coal and the rate of heating.

During gasification of peat, the gaseous phase contains alkalis primarily as chlorides and hydroxides of sodium and potassium [Muchmore et al., 1995; Olsson and Pettersson, 1998]. In fluidized-bed gasification both metals condense downstream as chlorides and a larger amount of both metals are released in the vapour phase during gasification than combustion [Mojtahedi and Backman; 1989; Muchmore et al., 1995]. High chlorine content enhances the volatilization of the alkali metals [Davidsson et al., 2002b; Muchmore et al., 1995; Olsson et al., 1997; Olsson and Pettersson, 1998; Sheldon et al., 1992]. An average of 11.9% of the potassium, and 20.7% of the sodium entered the gas phase under the gasification conditions studied by Muchmore et al. [1995], making sodium the major vapor-phase alkali (Na and K) species. Potassium in coal occurs largely as non-volatile aluminosilicates [Muchmore et al., 1995; Sheldon et al., 1992]. Under the conditions studied by Muchmore et al. [1995] it was found that the major portion of the alkali metals was retained in solid phases during gasification.

2.5.1 Catalytic Gasification

Coal gasification at moderate conditions can be achieved by the utilization of catalysts [Zhu et al., 2008]. A series of catalysts, including carbonates of alkali metals, have been tested on Shangwan coal (bituminous coal) and demineralized Blair Athol char [Nishiyama, 1991; Zhu et al., 2008]. Physical mixing of the catalyst with the coal was found to be less effective than impregnation, which is true in the case of catalysts such as calcium [Liu and Zhu, 1986]. Potassium carbonate for example has been found to have the same reactivity for either mechanically added catalyst or the impregnation of the catalyst [Liu and Zhu, 1986]. It was indicated by Nishiyama [1991] that the increase in reactivity can possibly be due to a change in surface area or chemical state change of the catalyst or catalyst-carbon system. Molten catalysts are better able to penetrate the coal structure and, hence, improve accessibility of the unavailable carbon sites in the interior of the coal/char [Sheth et al., 2003]. Wood et al. [1984] reported that alkali carbonates mixed with the coal will chemically interact with the char at sub-gasification temperatures to form a liquid phase in intimate contact with the char. This seems to be a prerequisite for effective performance of the additive as a catalyst for gasification of char [Wood et al., 1984]. According to Shadman

et al. [1987] potassium has a stronger interaction with graphitic substrates than sodium and is released more slowly than sodium to the gas phase (11.9% vs. 20.7%).

The reactivity of a catalyst loaded demineralized char was found to be higher than that of catalyst loaded raw char. The reason for this being that there are less catalyst poisons present in demineralized coal systems [Nishiyama, 1991]. Although demineralization can modify the chemical composition of the coal by increasing the volatile matter, oxygen and nitrogen content of the coal, it does have a better combustibility than the parent coal [Rubiera et al., 2002]. Three factors are the reason for rate change during the phase change of the catalysts. It is said to be: (1) catalyst vaporization, (2) catalyst migration on the surface, and (3) the increase in the carbon surface area due to conversion [Shadman et al., 1987].

2.5.2 Proposed Mechanisms of Alkali as Gasification Catalysts

The main mechanism of catalysis using alkali and alkaline earth metal salts in steam or carbon dioxide gasification involves the supply of oxygen from the catalyst to carbon, perhaps through the formation and decomposition of a C-O complex [Nishiyama, 1991; Shadman et al., 1987]. An essential initial step in the catalytic mechanism is a chemical interaction between the carbon and the inorganic salt to form a reactive intermediate [Wood et al., 1984]. When potassium carbonate was mixed with char, CO_2 emissions in the temperature range of 673 °C-773 °C suggested that the carbonate decomposed at these temperatures [Wood et al., 1984]. The catalyst thus dissociates molecular oxygen into atomic oxygen and this happens at a much faster rate than on an uncatalyzed coal surface. This mechanism was postulated to work through a redox cycle [Shadman et al., 1987; Suzuki et al., 1984]. During this mechanism the alkali catalyst cycles between an oxidized and a reduced form [Shadman et al., 1987] i.e. the catalyst transfers oxygen from the gaseous reactant to the carbon surface and the net effect being CO formation. These atomic oxygen molecules migrate to the carbon surface and then form carbon oxides such as CO and CO_2, thus oxygen transfer is proven to play a major role in catalysis [Nishiyama, 1991].

According to Kapteijn et al. [1986] the first step during gasification is an oxidation of the carbon surface. The catalyst only increases the concentration of these oxidized sites, but does not interfere with the second rate determining step. For the alkali catalyzed reaction the first step in the kinetic model also represents an oxidation of carbon free sites, probably in the vicinity of a catalyst species. Two combustion regimes are defined according to the

rate-limiting step in the process: (1) the diffusion of oxygen into the pore network of the char, and (2) the diffusion of oxygen across a boundary layer surrounding the outer surface of the particles [Alvarez and Borrego, 2007]. Two types of oxidic species are present during alkali metal catalysed gasification in CO_2: (1) surface bonded –OM species of high stability and (2) oxidic species having a lower interaction with the carbon [Kapteijn et al., 1984].

It was proposed by Takarada et al. [1986] that potassium carbonate decomposes and forms a surface intermediate, K-O-C, and thus potassium is atomically dispersed onto the carbon surface. It was also claimed to be probable that the potassium carbonate would react with carbon in coal during devolatilization under 800 °C and in a N_2 atmosphere [Liu and Zhu, 1986]. Thus, this will reduce the potassium carbonate to metallic potassium of low melting point, which makes the catalyst mobile and highly dispersed onto the char surface.

According to McKee [1983] a re-distribution of π-electrons in the carbon structure may be caused by the presence of a catalyst. This is the result of transfer of electrons to or from the carbon substrate. There is a weakening of the C-C bonds at the edges of the graphite sheets and an increase in the C-O bond strength during oxidation. It was also suggested by McKee [1983] that alkali metal atoms on the carbon surface act as sites for the chemisorptions of oxygen, thus weakening the C-C surface bonds and promoting the desorption of gaseous oxidation products at low temperatures. Adsorbed alkali metal atoms may alter the ionization potential of the surface carbon atoms. Thus, the catalytic effects of alkali metals salts on the gasification reactions of carbon appear to be best explained by sequences of cyclic redox processes involving reaction of the salts with the carbon substrate and subsequent re-oxidation by reaction with the oxidizing gaseous environment.

Wood et al. [1984] suggested that at elevated temperatures in the presence of carbon, alkali metal carbonates are chemically converted to oxides containing an excess of the alkali metal. At gasification temperatures, the oxide melts to form a liquid film that spreads over the carbon surface. Apart from quartz, all mineral species decompose and leave a large amorphous mass of oxides [Kühn and Plogmann, 1983]. These decompositions result in the mineral matter being in a very reactive state.

It was reported by Chen and Yang [1997] that there have been many propositions for intermediate states for potassium during gasification which include: K, K_2O, K_2O_2, K_2CO_3, K-O-C and clusters which are non-stoichiometric compounds with excess metal. Among all these proposed intermediates, clusters (or particles) are the most active species. Chen and Yang [1997] proved in their study that the C-O-K group has only little catalytic activity as

compared to catalyst particles and clusters. The generally postulated mechanism consists of an oxidation-reduction cycle in which oxygen is transferred to the carbon active sites through the catalytically active alkali and alkaline earth species, followed by the liberation of CO from the active carbon-oxygen complexes. The last step is considered rate-limiting.

The main difficulty in a catalytic gasification reactor involves the degree of contact between the coal and the catalyst. When the catalyst is simply mixed and introduced into the system, the degree of contact is generally poor until the catalyst has melted in the reactor [Sheth et al., 2003]. The pre-addition of catalyst to the char ensures good catalyst contact. The increase in reactivity of coal after addition of potassium carbonate might not be because of a decrease in the activation energy, but from an increase in the density of the reactive sites [Audley, 1987]. For a catalyst to function satisfactorily in carbon or char, a three-phase interface must be maintained between the carbonaceous substrate, the catalyst phase and the gaseous oxidant as mentioned before [Sheth et al., 2003]. Whatever the detailed mechanism of the catalytic process are, the overall rate of gasification should be enhanced by improving the contact between the catalyst and carbon as long as the gaseous oxidant still has easy access to this interface [Sheth et al., 2003].

Out of the proposed mechanisms it can be concluded that the alkali metal does not necessarily increase the reactivity, but increases the availability of oxygen to the carbonaceous substrate, which in turns increases the reactivity. The alkali metal carbonates melt and decompose below gasification temperatures and is evenly distributed throughout the coal matrix, without blocking the pores. Thus a C-O-M interface is formed, which improves the oxygen supply to the coal matrix and in turn increases the gasification rate of the coal.

2.6 Char

Devolatilization of coal refers to the decomposition of organic matter by heat in the absence of air [Probstein and Hicks, 2006]. When coal is devolatilized, hydrogen-rich volatile matter is distilled and a carbon-rich solid residue is left behind. The carbon and mineral matter that remain behind are the residual char [Probstein and Hicks, 2006]. The devolatilization of the coal increases the porosity of the char. As seen in most of the literature char gasification undergoes the same processes as coal gasification. It was proved by Adánez et al. [1985] that demineralized char has lower reactivity than untreated char, but

passes through a maximum on a curve which is typical of the gasification of a porous solid with pore enlargement. The big difference in the thermal treatment of these two compounds is whether the catalyst is added before or after charring of the carbon. As mentioned by Chen and Yang [1997], the rate limiting step in adding alkali carbonate catalysts to the coal or char is the decomposition of the carbonate and the melting of the catalyst which helps in evenly distributing the catalyst. Spiro et al. [1984] found that differences are expected in pre- and post catalyzed char reactivity as chars are structurally rigid when catalysts are added, whereas raw coal retains some plastic properties that may influence catalyst distribution and contacting during devolatilization. Their experiments also showed that it matters little if the catalyst is pre- or post added to the char. The particle size of the sample used for this analysis were approximately 500 μm and the catalysts added was 5% Li_2CO_3, 5% Na_2CO_3, 5% K_2CO_3, 20% Li_2CO_3 added to Illinois No 6 bituminous coal and 5% K_2CO_3 added to Navajo sub-bituminous coal as weight percentage.

Physical and chemical characterizations are done to determine the effect the mentioned properties of coal have on reactivity or gasification rate. The techniques performed on the samples are discussed in Chapter 3.

Chapter 3

Characterization Techniques

3.1 Overview

Coal characterization techniques have many benefits for understanding coal and coal char, but coal is difficult to be characterized because it is an extremely complex heterogeneous material. It is also composed of a number of distinct organic entities called macerals and lesser amounts of inorganic substances known as minerals [Crelling, 2009]. Macerals in minerals occur in distinct associations called lithotypes. Each lithotype has a unique set of physical and chemical properties, which also affect coal behaviour [Crelling, 2009].

The basic units in which coal occurs, is in coal seams which are composed of coal lithotypes; and individual coal seams may have their own set of physical and chemical properties [Crelling, 2009]. With the same mineral and maceral composition, there can be different sets of properties because the lithotypes are not necessarily the same. There are thus a number of levels of characterization of the coal. This includes characterization of the macerals, the lithotypes, the entire seam and the association of the seam with its enclosing strata [Crelling, 2009].

In this chapter a literature background is given on the mineralogical, chemical and physical analytical techniques done on the samples during this study. The analytical techniques include:

- XRD;
- QEMSCAN;
- Proximate;
- Ultimate;
- XRF;
- Ash Fusion Temperature;
- Carbon Dioxide BET Surface Area Measurements.

3.2 X-ray diffraction (XRD) Analysis

X-ray diffraction is a rapid analytical technique primarily used for phase identification of the fine structure of crystalline material [Cullity, 1959]. Using pure and known lattice spacing of crystal samples, the XRD apparatus is calibrated to determine the unknown samples' crystal lattice spacing [Huggins, 2002; Ward, 2002]. A crystal lattice is a solid, regular array of positive and negative ions [Kotz and Treichel, 2003]. According to Nuffield [1966] an electron in the path of an unpolarized X-ray beam vibrates with the frequency of the incident radiation, periodically absorbing energy and emitting it as X-radiation. The original X-rays are unmodified in wavelength by the interaction but are reflected in all directions [Nuffield, 1966]. The electron thus has the effect of scattering the incident radiation and acts as a source of secondary X-rays and all atoms in the path of an X-ray beam scatter X-rays simultaneously. The co-operative scattering is known as diffraction [Nuffield, 1966]. XRD analyses on coal samples are semi-quantitative [Huggins, 2002; Ward, 2002]. The Rietveld [1969] method was developed to improve XRD analysis on raw coal samples because of the complications caused by the amorphous carbon in the coal [Huggins, 2002]. Figure 3.1 shows a typical XRD instrument.

Figure 3.1: A typical XRD apparatus. The apparatus shown in the figure is Bruker's X-ray diffraction D8-Discover instrument.

3.3 QEMSCAN

QEMSCAN is an abbreviation for Quantitative Evaluation of Minerals by Scanning Electron Microscopy [Creelman and Ward, 1996; Galbreath et al., 1996; Grigore et al., 2008; Liu et al., 2005; Van Alphen, 2007; Ward, 2002]. It is a combination of scanning electron microscopy (SEM) and electron probe microanalyzer (EPMA) and this combination is used to produce an image of individual coal particles as well as their chemical associations [Liu et al., 2002, Ward, 2002]. The sample preparation has a few steps before analysis can start. During step one the use of splitting and riffling is necessary to obtain a representative sample. These samples are mixed with graphite then mounted in Araldite epoxy-resin and allowed to cure. The samples in Araldite epoxy-resin are then carefully polished to a diamond finish of 1 µm. The types of samples that are analyzed using this technique are mostly rock- and ore-forming minerals. The images that are formed are built up using the identified chemical species that is in each pixel [Gupta, 2007; Liu et al., 2005; Ward, 2002]. QEMSCAN is a suitable method to determine the abundance or distribution of mineral species present in the sample or sample ash [Gupta, 2007; Liu et al., 2005].

Figure 3.2: A photo of an Intellection QEMSCAN apparatus.

3.4 Proximate Analysis

Proximate analysis is formally defined by a group of ASTM test methods [Donahue and Rais, 2009]. Proximate analysis defines the fraction of moisture, volatile matter (consisting of gases and vapors generated during pyrolysis), fixed carbon (which is the non-volatile fraction of coal), and ash (which is the residue remaining after combustion)

[Probstein and Hicks, 2006]. These are important properties of coal [Probstein and Hicks, 2006]. Before obtaining the proximate analysis data, the wet coal should be air dried at 10-15 °C above ambient temperature; otherwise the coal could be too wet to crush [Probstein and Hicks, 2006]. The coal is then crushed and dried again in a forced-air circulation oven at 105 to 110 °C under nitrogen [Donahue and Rais, 2009]. The total moisture is then recorded as the sum of the mass losses from the air-drying and oven-drying processes [Probstein and Hicks, 2006].

During the next step after moisture determination, the coal is heated in a covered crucible under nitrogen for about 7 minutes to a temperature of about 950 °C and the further loss in mass is recorded as the volatile matter [Donahue and Rais, 2009; Probstein and Hicks, 2006]. The volatile matter primarily consists of tar, lighter oils, hydrocarbon gases, hydrogen, oxides of carbon, and water as decomposition products of the coal.

During the final phase, the coal is oxidized and the loss in mass is known as the fixed carbon content. The solid residue remaining is known as ash, the inorganic mineral matter, and any contamination from mining [Probstein and Hicks, 2006].

3.5 Ultimate Analysis

The term ultimate analysis refers to the determination of the concentration or proportion of every element in a compound without regard to (or without knowing) the compound's structure [Schobert, 2008]. Ultimate analysis is the determination of the percentages of the five most abundant elements in coal: i.e. carbon, oxygen, nitrogen, hydrogen and sulphur [Probstein and Hicks, 2006]. This is especially important to coal because the molecular structure is not specifically known [Schobert, 2008]. Usually carbon, hydrogen, nitrogen and sulphur are determined directly and oxygen is determined by difference because of the difficulty to determine it directly [Schobert, 2008].

3.6 X-ray fluorescence (XRF) Analysis

XRF provides the means for the identification of an element by measurement of its characteristic X-ray emission wavelength or energy [Günzler and Williams, 2002]. According to Bauer et al. [1978] X-ray fluorescence, also known as secondary X-ray emission involves the sample being bombarded with an X-ray beam and the re-emitted X-radiation is measured. An X-ray fluorescence spectrometer needs an X-ray source, a means of

dispersing the X-rays, and a detector. A very wide range of samples in various forms can be analyzed by XRF, from ash and powders to films and sheets. Quantitative analysis is achieved by comparing intensities from unknowns to those from primary or secondary standards. The method is generally non-destructive, therefore the sample can be retained for other analyses [Bauer et al., 1978; Dzubay, 1978]. Figure 3.3 is a typical XRF instrument used for these analyses.

Figure 3.3: A Philips PW 1606 X-ray fluorescence spectrometer with automated sample feed.

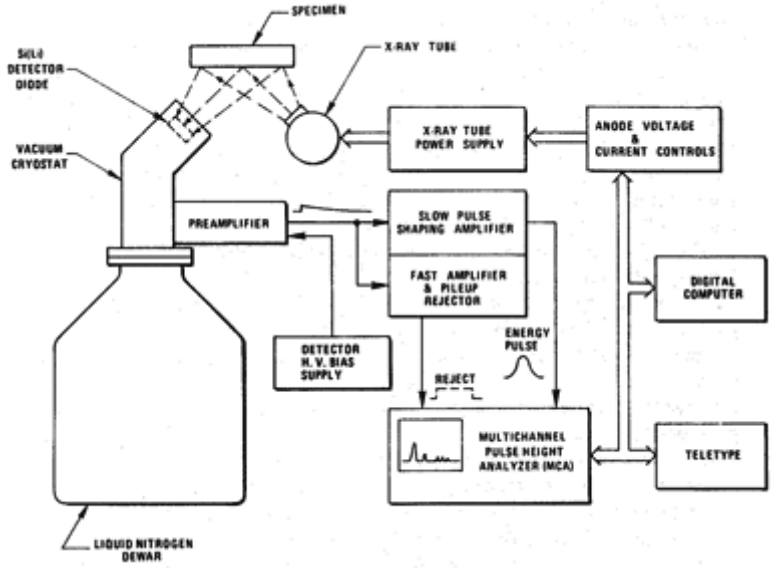

Figure 3.4: A block diagram of a typical energy dispersive X-ray fluorescence (EDXRF) spectrometer [Taken from Jenkins et al., 1995].

Figure 3.3 is a photo of a standard XRF apparatus. In Figure 3.4 a block diagram of a typical EDXRF spectrometer is depicted. In Figure 3.4 the entire polychromatic spectrum from the sample is incident upon a detector that is capable of registering the energy of each photon that strikes it. The detector electronics and data system then compile the X-ray spectrum as a histogram, with number of counts versus energy [Guthrie, 2010].

3.7 Ash Fusion Temperature (AFT)

Ash fusion temperature is the temperature at which melting of the ash is initiated [Song et al., 2010; Weeber et al., 2000]. Ash fusion temperature measurements are used as a guide to the clinkering behaviour of coal ash in furnaces using a laboratory determination [Lloyd et al., 1993; Zhao et al., 2010]. It is used to predict the slagging potential of coals fired in pulverized coal utility boilers [Lloyd et al., 1993; Zhao et al., 2010]. Ash fusion temperature is the temperature at which controlled heating of the ash under oxidizing conditions causes sufficient softening to change a moulded pyramid shape ash pellet to a hemispherical shape (height equal to half the base), which represent only one of four required temperatures [Lloyd et al., 1993]. During this test a prepared pyramid shape of the ash is placed in a furnace and heated at approximately 5 to 10 °C/min from 1000 °C to 1600

°C [Wall et al., 1998, 1999]. The reason for the use of oxidizing conditions is to compare the results of two samples.

There are four different temperatures which are measured during ash fusion temperature analysis; (1) initial deformation temperature (IDT or DT), (2) spherical or softening temperature (ST), (3) hemispherical temperature (HT) and (4) flow or fluid temperature (FT) [Lloyd et al., 1993; Zhao et al., 2010]. These four temperatures can be determined using the instrument illustrated in Figure 3.5.

- **Initial deformation temperature**: This is the temperature where ash begins to fuse or deform. Where the tip of the cone or pyramid rounds [ICT, 2006; Zhao et al., 2010].
- **Spherical or softening temperature**: This is also known as the fusion temperature where the height of the cone and the width of the base are equal. Here is a transition between initial deformation and fluidity [ICT, 2006; Zhao et al., 2010].
- **Hemispherical temperature**: The temperature where the height of the cone is equal to half of the base. It is almost a molten liquid [ICT, 2006; Lloyd et al., 1993; Zhao et al., 2010].
- **Flow of fluid temperature**: The ash has melted to a molten liquid [Zhao et al., 2010].

Figure 3.5: A photo of an ash fusion determinator.

3.8 Carbon Dioxide BET Surface Area Measurements

The BET method was developed by Stephen Brunauer, P.H. Emmett and Edward Teller as a mathematical method to determine the micropore surface area of samples

[Brunauer et al., 1938]. The BET equation is used to determine the surface area from the physical adsorption of a gas on a solid surface [Hill, 1996]. CO_2 BET is used to determine the micropore surface area by making use of the solubilisation mechanism [Amarasekera et al., 1995]. Narrower pores are not accessible to nitrogen at the low temperatures of analysis, while CO_2 at 0 °C can penetrate most of the pores [Valix and Trimm, 2000]. Pores in coal are isolated from each other and the efficiency of carbon dioxide as an adsorbate is the result of its ability to diffuse rapidly through the solid coal. It thereby reaches all the pores, including those regarded as not having surface openings [Amarasekera et al., 1995]. The surface area of these micropores of Highveld coal was determined using a Micrometrics ASAP 2010 analyzer depicted in Figure 3.6.

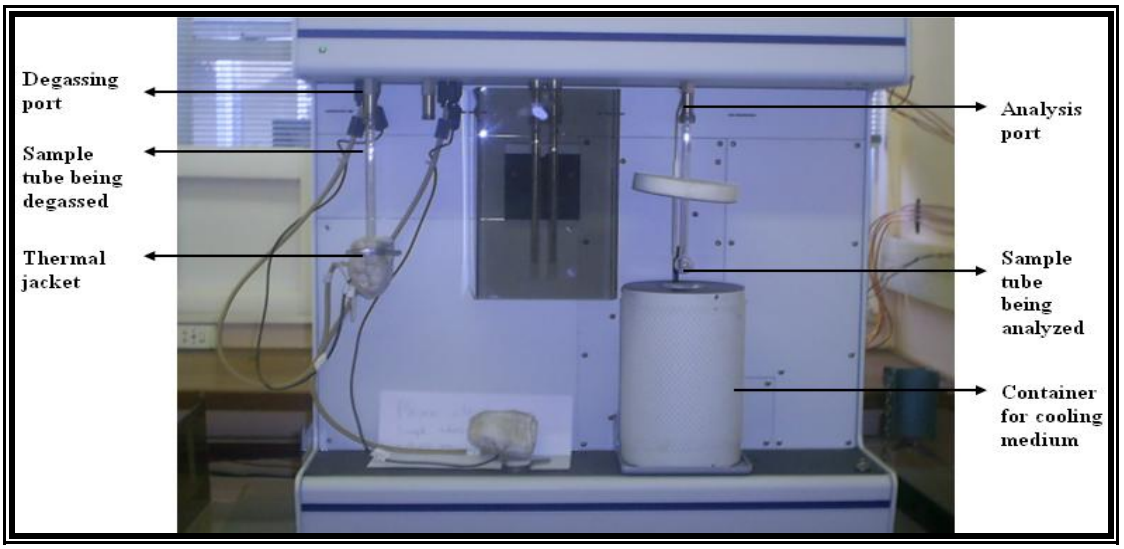

Figure 3.6: A photo of the Micrometrics ASAP 2010 analyzer at the North-West University, Potchefstroom Campus.

Chapter 4

Experimental Methods

This study focussed mainly on the effect of catalyst addition to coal and char, respectively. To limit the variables during the research the coal was demineralized to remove the influence of the some mineral matter. In this chapter the experimental methods used in this study are discussed in detail. The experiments were performed in a temperature range that is easy to duplicate on a laboratory scale. The temperature range is between 500 °C to 900 °C. The sample preparation, which includes screening and demineralization, is followed by compositional analysis. Methods used to investigate the mass loss of the coal/char during thermal treatment in CO_2 of the samples included: ash percentage determination, proximate analysis, ultimate analysis, ash fusion temperature, X-ray diffraction, X-ray fluorescence, carbon dioxide BET analysis and QEMSCAN.

4.1 Materials

A high-inertinite, high-ash, Highveld bituminous coal was used for the research. The coal has an ash content of 26.2% as seen in the proximate analysis and confirmed by the ash percentage results obtained. It is also supported by Van Niekerk et al. [2008]. The coal was crushed and screened to obtain 100% passing of 75 µm particles. The chemicals and gases as well as the grade that were used during the study are given in Table 4.1.

Table 4.1: Chemicals/gases including their grade used during the study.

Chemicals/Gases	Grade
Anhydrous Potassium Carbonate	Analytical grade supplied by ACE Chem.
Anhydrous Sodium Carbonate	Analytical grade supplied by ACE Chem.
32% Hydrochloric Acid	Analytical grade supplied by ACE Chem.
48% Hydrofluoric Acid	Analytical grade supplied by ACE Chem.
Nitrogen	Analytical grade supplied by Afrox.
Carbon Dioxide (Wet)	Analytical grade supplied by Afrox.

The anhydrous potassium carbonate and sodium carbonate were crushed before use to ensure effective distribution of the catalyst in the coal sample. Before addition of the catalysts they were first dried in a furnace at 100 °C to remove hygroscopic water. The X-ray fluorescence results of the catalysts to determine the purity is given in Chapter 5, Section 5.5, Table 5.4.

4.2 Screening and Demineralization

A typical inertinite-rich, high-ash South African Highveld coal was crushed and screened to obtain a 100% passing of 75 µm particles. Some of the parent coal was removed and stored in a desiccator under nitrogen for further comparison of the changes that occur. The rest of the coal was demineralized for further analyses and treatment.

The coal was demineralized using a harsh hydrochloric/hydrofluoric/hydrochloric acid leaching method developed by Van Niekerk et al. [2008]. 5M hydrochloric acid was added to the coal sample and stirred with a polyethylene magnet in a glass beaker for 24 hours. The stirrer was switched off for an additional hour before decanting and filtering the sample. The coal cake was returned to a polyethylene beaker and 48% (28.9M) hydrofluoric acid was added. The mixture was then stirred for 24 hours. The stirrer was switched off for an additional hour after stirring before carefully decanting and filtering the sample until dry. The filter cake was returned to a glass beaker and 5M hydrochloric acid was again added to the coal. The mixture was stirred for 24 hours. The stirrer was switched off for an additional hour before decanting and filtering the mixture. The coal cake was then thoroughly washed with distilled water until a constant pH was obtained and filtered until dry. The coal was then dried under vacuum at 60 °C for not less than 12 hours and stored in a desiccator under nitrogen in a dark place until use. The complete demineralization procedure was done at ambient temperature in an acid fume hood at all times.

For every 100 g of sample used, 400 ml of acid was used until enough demineralized sample was obtained. About 30% of total sample mass is loss after demineralization and drying of the coal. It is possible that the mass loss after demineralization can be up to 50% because the samples are not dried before the demineralization process. Thus the extra mass lost was probably moisture. The total demineralized sample was quartered and coned to obtain representative samples. The quarter and cone method is as follows:

- The sample is placed on a clean surface (concrete or steel mixing sheet) and mixed thoroughly by transferring the coal from one point to another by using a spoon,

always putting the spoonful of material on top of the cone. This step should be and was repeated three times.

- Now the coal should be flattened with a shovel and divided into four quarters. A suitable device should be constructed to obtain better results.
- The opposite quarters should be rejected.
- The two remaining quarters should be mixed again using the same starting procedure.
- The process should be repeated until the desired amount of sample is achieved [TSACPS, 2002].

The results of the proximate and ultimate analyses of the raw and demineralized coal are given in Chapter 5, Section 5.1.

4.3 Coal Characterization

To determine the ash content of the coal sample used for the research, the ISO 1171 method was used [TSACPS, 2002]. Approximately one gram of coal is weighed into a sample holder of known weight and placed into a furnace at ambient temperature. The furnace is ventilated with air. The temperature is then slowly raised to 800 °C and maintained for a fixed period of time. The sample holder is removed from the furnace, cooled in air and then placed into a desiccator, and the mass of ash in the sample holder is determined. The mass of ash, expressed as a percentage of the weight of the coal used, is the ash content. The method was taken from The Coal Processing Society of South Africa [2002] and was performed on the raw coal as well as the demineralized coal.

Proximate, ultimate and ash fusion temperature analyses were performed. Proximate analyses were performed on the demineralized and raw coal samples, on a dry air basis, using several standard methods listed below. The apparatus that was used for this analysis is a Series 2000 furnace.

Table 4.2: Methods used to determine the composition of coal.

Fraction Analyzed	Method used
Inherent Moisture	ISO 589 [SABS ISO; 2009]
Ash	ISO 1171 [SABS ISO; 2010b]
Volatile matter	ISO 562 [SABS ISO; 2010a]
Fixed Carbon	By difference
Total Sulphur	ASTM D4239 [ASTM; 2010]

Carbon, hydrogen and nitrogen were determined by ASTM D5373 [ASTM; 2008] in the ultimate analyses. Total sulphur was determined by ASTM D4239 [ASTM; 2010] and oxygen was determined by difference. The apparatus that was used for the ultimate analysis is a Truspec ultimate analysis apparatus.

Ash fusion temperatures were performed on the demineralized and raw coal using the ISO 540 method under oxidizing conditions. The apparatus used in determining the ash fusion temperatures is an Elite Ash Fusion Temperature apparatus.

4.4 X-ray diffraction and X-ray fluorescence

XRD and XRF analyses were all performed by Setpoint Laboratories using accredited analysis methods for determining the species in the samples. The laboratory is the SANAS (South African National Standards) Testing Laboratory No. TO223. The ISO 17025 [2006] method for silicate analysis is accredited by SANAS. These analyses were performed to test the purity of the ash of the char, as well as prepared ash samples of the demineralized coal and the salts to test the purity of the catalysts.

The instrument used for the XRD analysis was a Thermo-Fischer ARL X-tra. The analyses were performed under ambient atmosphere, laboratory pressure, laboratory temperature and relative humidity conditions. The preparation method involves a finely pulverized material and the undiluted powder is manually inserted in a sample holder.

The instrument used for the XRF analysis is a ThermoARL model 9800XP simultaneous/sequential XRF. All of the inorganic elements present in the powdered samples can be accurately detected by XRF including Na, Cl and S. The XRF technique used in this study is regarded as only semi-quantitative for the Na, Cl and S.

4.5 Thermal Treatment Experiments

A muffle furnace with a gas inlet was used for charring and gasifying the samples. Nitrogen was used as atmosphere for charring and CO_2 for gasification. Demineralized coal placed in a porcelain crucible was placed into the muffle furnace. The sample was heated to 900 °C with a nitrogen flow of 100 cm^3/min. The sample was left in the furnace under these inert conditions for a fixed period of time. In this case, 3 hours at 900 °C, was sufficient.

Different concentrations (0.25%, 0.5%, 0.75%, 1%, 2% and 4%) of potassium carbonate, sodium carbonate and a 1:1 mixture (wt%) of the two catalysts were added to the coal and char samples. Porcelain crucibles were burned clean at 1000 °C in a muffle furnace and then weighed after it cooled to ambient temperature. The mass was noted and approximately 300 mg of the prepared coal and char samples were weighed into each. These samples were placed in the furnace and flushed with CO_2. A constant flow of 50 cm^3/min of CO_2 was maintained while the furnace was heated to 500 °C. The samples were kept in the furnace for 120 minutes, which included the time necessary to reach 500 °C. After 120 minutes the crucibles were removed from the furnace and placed in a desiccator to cool down to ambient temperature. The crucibles were weighed and placed in the muffle furnace again. The same procedure was followed for the 600 °C, 700 °C, 800 °C and 900 °C experiments. At 900 °C the samples were left in the furnace for 10 hours then carefully removed from the furnace and placed in a desiccator to cool to ambient temperature. The samples were then weighed for a last time. The experiments were performed in triplicate for repeatability. The mass losses of each were noted and an average value for the three sets was determined. The interim results were not used for the explanation of this study, because the results obtained was not clear enough to explain the difference in pre- and post-addition of catalyst to char. It was thus used to ensure that all samples were treated in a similar way.

Regular TGA experimental work could unfortunately not be performed because of technical difficulties occurring during the study.

4.6 Carbon Dioxide BET Analysis

The CO_2 BET analyses were done using the Micrometrics ASAP 2010 Analyzer at the North-West University. 0.2 g of sample was placed in a glass tube, degassed at 25 °C for a 48 hour period and then analyzed via carbon dioxide adsorption at 0 °C. The Dubinin-

Radushkevic method for micropore surface area determination was used to measure the surface area of the raw coal, demineralized coal, char at 700 °C and 900 °C, as well as demineralized coal with 4wt% added potassium carbonate charred at 700 °C and 900 °C. The experiments were done in duplicate for repeatability and the standard deviation for the results given by measurements on the apparatus was ± 4.6 g/m^2.

4.7 QEMSCAN

QEMSCAN was performed on the demineralized char sample, pre-added 4% potassium carbonate to char and pre-added 4% sodium carbonate to char. Post-added 4% potassium carbonate to char was ashed and sent for analysis. The catalysts were also sent for QEMSCAN analysis for comparison reasons. The polished sections of samples were prepared using Carnauba wax. The QEMSCAN used, is a configured scanning electron microscope (SEM) to automatically determine the mineralogical composition and particles characteristics of the chosen samples.

Chapter 5

Results and Discussion

Demineralization, drying and catalyst addition may have an effect on the possible mass loss of the coal samples during CO_2 thermal treatment. Several analyses and experiments were performed to determine the extent of the effect. This chapter includes all the analyses done on the catalyzed and uncatalyzed coal/char samples to better investigate what happens during gasification. The mass loss during thermal treatment of the coal and char samples are represented in bar graphs to better compare the results obtained.

5.1 Ash Percentage Determination and Proximate Analysis

After following the procedure explained in Section 4.3, the final masses were obtained and the ash yield of the raw coal and the demineralized coal were 27% and 2%, respectively. This corresponds well with the results obtained from the proximate analysis given in Table 5.1.

Table 5.1 shows the normalized data of the raw/parent coal, as well as the demineralized coal on an air dried basis, moisture free basis and dry ash free basis (DAF). It can be observed from Table 5.1 that the demineralization procedure was effective in removing 93% of the ash present in the raw coal. It corresponds well with the results of Van Niekerk et al. [2008]. During their study the same process removed 92.4% minerals from their coal sample. It was determined using the following formula:

100% - [(1.8/26.2)*100%] = Percentage minerals removed

It can thus be assumed that most of the inherent minerals that may have an influence on the experiments were successfully removed (from 26.2% to 1.8%). McKee et al. [1983] found that mineral impurities can adversely affect the reactivity of the catalysts.

Table 5.1: Proximate analysis of raw coal and demineralized coal.

Analysis	Air Dried (%)		Moisture Free (%)		Dry Ash Free (%)	
Proximate	**Raw Coal**	**Demin* Coal**	**Raw Coal**	**Demin* Coal**	**Raw Coal**	**Demin* Coal**
Inherent H_2O	4.9	0.5	0	0	0	0
Ash	26.2	1.8	27.6	1.8	0	0
Volatile Matter	21.2	26.0	22.3	26.1	30.77	26.6
Fixed Carbon	47.7	71.7	50.2	72.1	69.23	73.4
Total Sulphur	0.63	1.03	0.63	1.03	0.63	1.03

* Demin = Demineralized

5.2 Ultimate Analysis and Ash Fusion Temperature Test

The normalized data of the ultimate analyses for raw and demineralized coal, as well as the ash fusion temperatures for the same samples are given in Table 5.2. According to the standard method for ash fusion temperature determinations, ash fusion temperatures are reported as rounded to the nearest 10 °C following rounding rules.

In the ultimate analysis results depicted in Table 5.2 it can be seen that the demineralization hardly had any effect on the carbon, hydrogen, nitrogen or oxygen content of the coal. The sulphur is approximately half of its original content as can be seen in Table 5.1. According to the ultimate analysis results it seems that the sulphur content doubles, but in reality the total amount of sulphur does not increase, the fraction relative to the remaining minerals increases. Almost all the sulphur can potentially be organically bound, and the demineralization reduces the mass base without removing a significant amount of sulphur. Larsen et al. [1989] supports that demineralization hardly has any effect on the macromolecular composition of coal as also seen in Table 5.2.

The ash fusion temperature results in Table 5.2, indicate that there was a c.a. 100 °C drop in all the fusion temperatures from the raw coal to the demineralized coal. This was due to the removal of the clays during the hydrofluoric leaching step of the demineralization procedure [Weeber et al., 2000]. The removal of clays (included mineral and extraneous minerals) from the coal during the demineralization process may contribute little to the lower AFT of the demineralized coal. But the fluxing elements-bearing minerals (dolomite, calcite, and pyrite) that are associated with the submicron clays in the coal macerals are responsible for the lower AFT of the demineralized coal. These fluxing elements (Ca, Fe, and Mg) remained in the demineralized coal and subsequently reacted with the submicron clays

and the organically-bound inorganic elements to form a melt during the AFT analysis. They also increase the basic oxide levels and lower SiO_2/Al_2O_3 ratios [Matjie et al., 2011; Matjie, 2008].

Table 5.2: Normalized data of the ultimate analysis and ash fusion temperatures for demineralized coal and raw coal.

Analysis	Raw (%)	Demineralized (%)
Ultimate		
Carbon	80.17	79.61
Hydrogen	3.72	3.29
Nitrogen	2.05	2.03
Total Sulphur	0.91	1.05
Oxygen	13.15	14.02
Ash Fusion Temperature (Oxidizing)	**(°C)**	**(°C)**
Initial Deformation Temperature (DT)	1350	1230
Spherical Temperature (ST)	1360	1250
Hemispherical Temperature (HT)	1380	1270
Flow Temperature (FT)	1400	1300

5.3 Thermal Treatment

5.3.1 Repeatability

Figures 5.1 to 5.6 show the repeatability of the thermal treatment experiments of char and coal with added 0.25% Na_2CO_3, 0.25% K_2CO_3 and 0.25% of the two catalyst mixture. The repeatability was very good considering that coal is very heterogeneous. The largest standard deviation on the experiments was approximately 3% when a triple set of experiments were performed. The thermal treatment method developed was thus successful when observing the repeatability results. The smooth lines fitted in the graphs are simply to increase readability of the figures. It is not the actual data points obtained during the study.

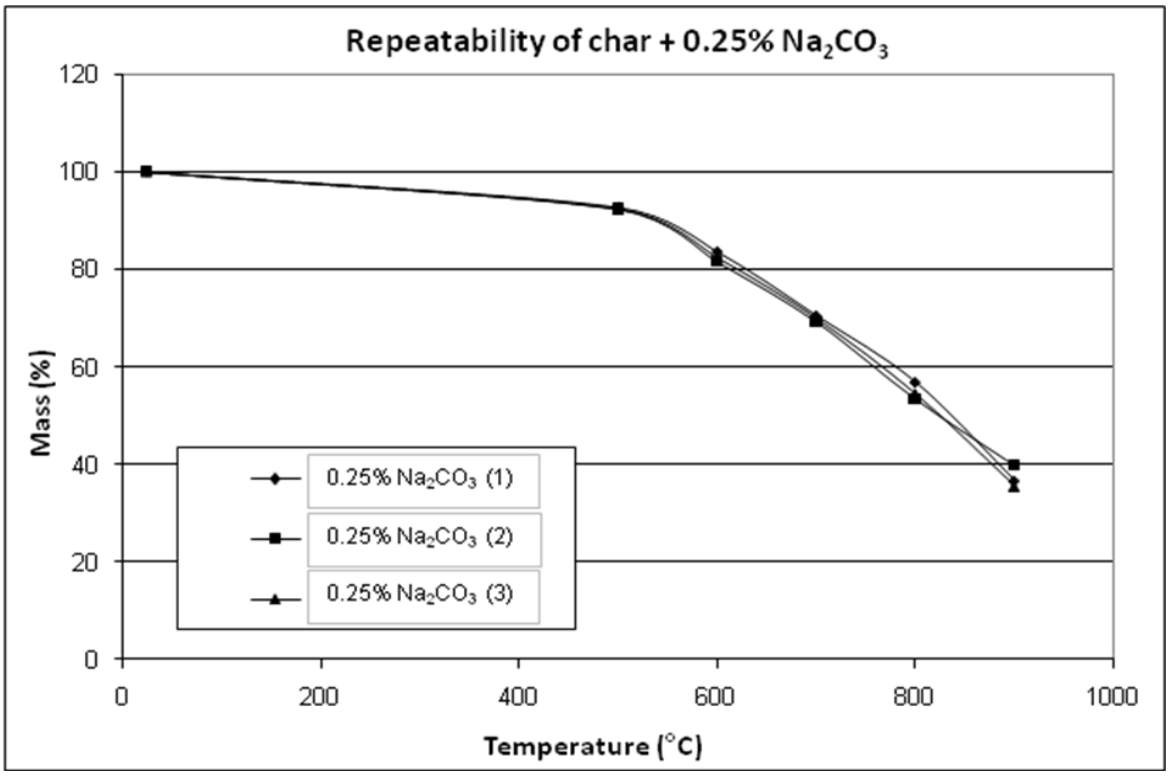

Figure 5.1: Repeatability of the mass loss of char with post-added 0.25% Na_2CO_3 during thermal treatment under CO_2.

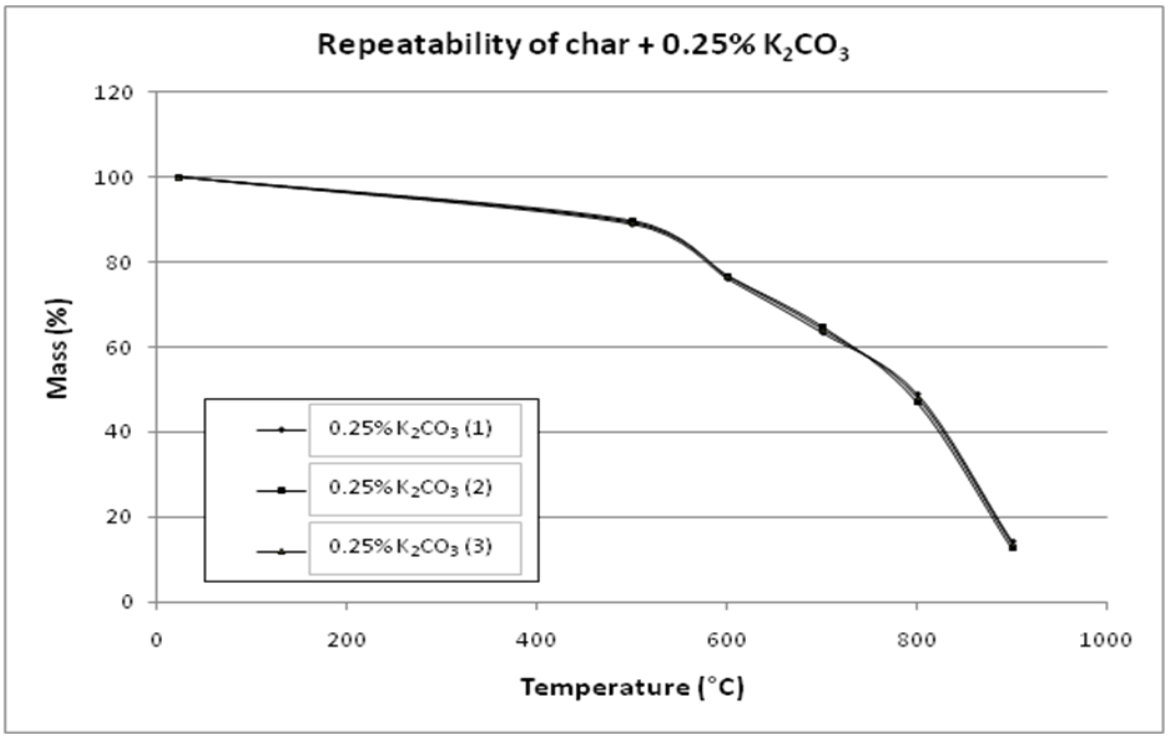

Figure 5.2: Repeatability of the mass loss of char with post-added 0.25% K_2CO_3 during thermal treatment under CO_2.

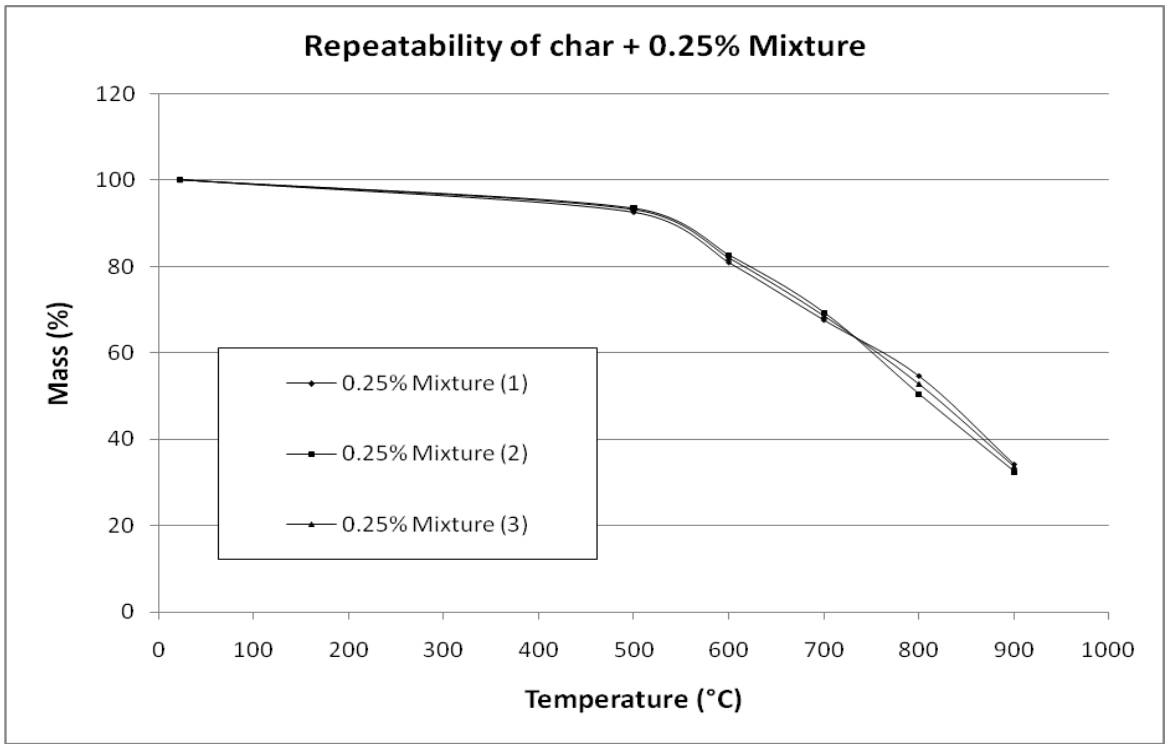

Figure 5.3: Repeatability of the mass loss of char with post-added 0.25% mixture of Na_2CO_3 and K_2CO_3 during thermal treatment under CO_2.

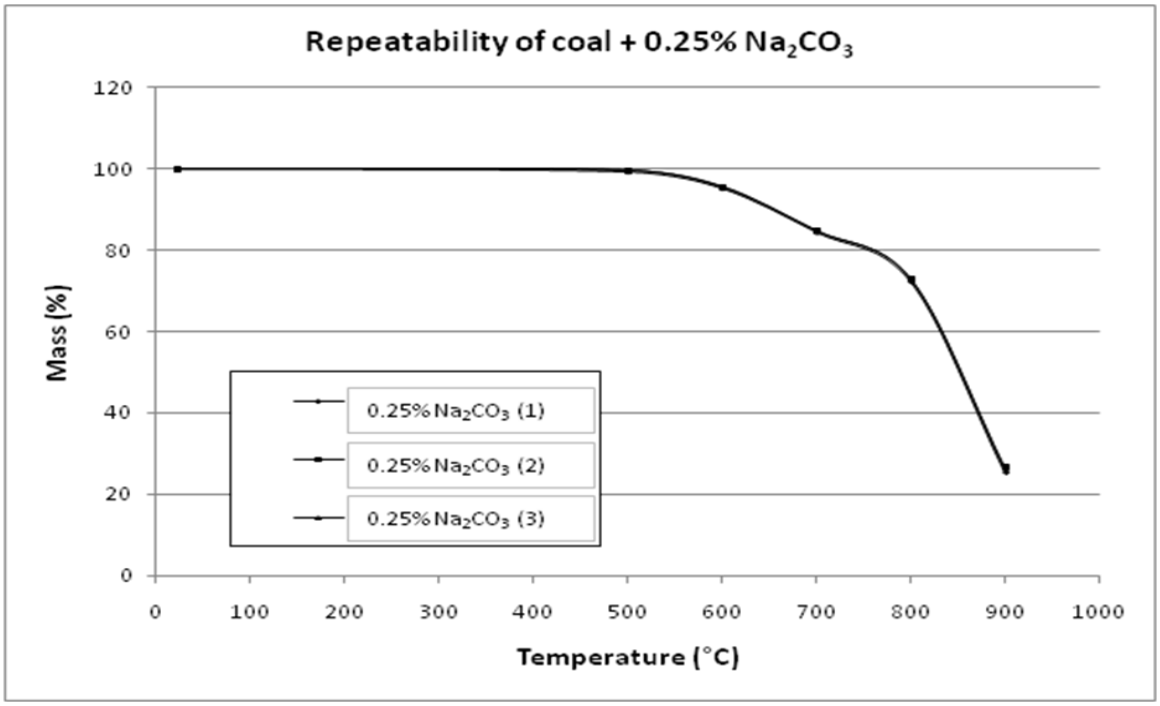

Figure 5.4: Repeatability of the mass loss of char from coal with pre-added 0.25% Na_2CO_3 during thermal treatment under CO_2.

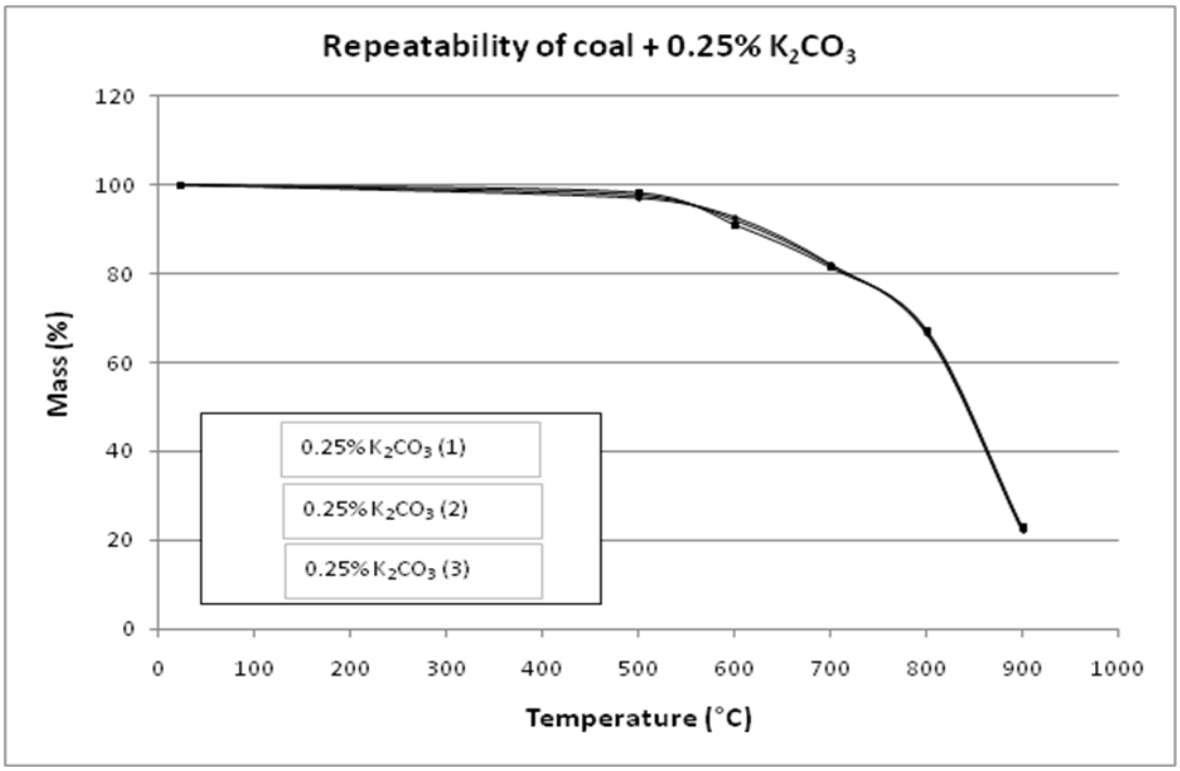

Figure 5.5: Repeatability of the mass loss of char from coal with pre-added 0.25% K_2CO_3 during thermal treatment under CO_2.

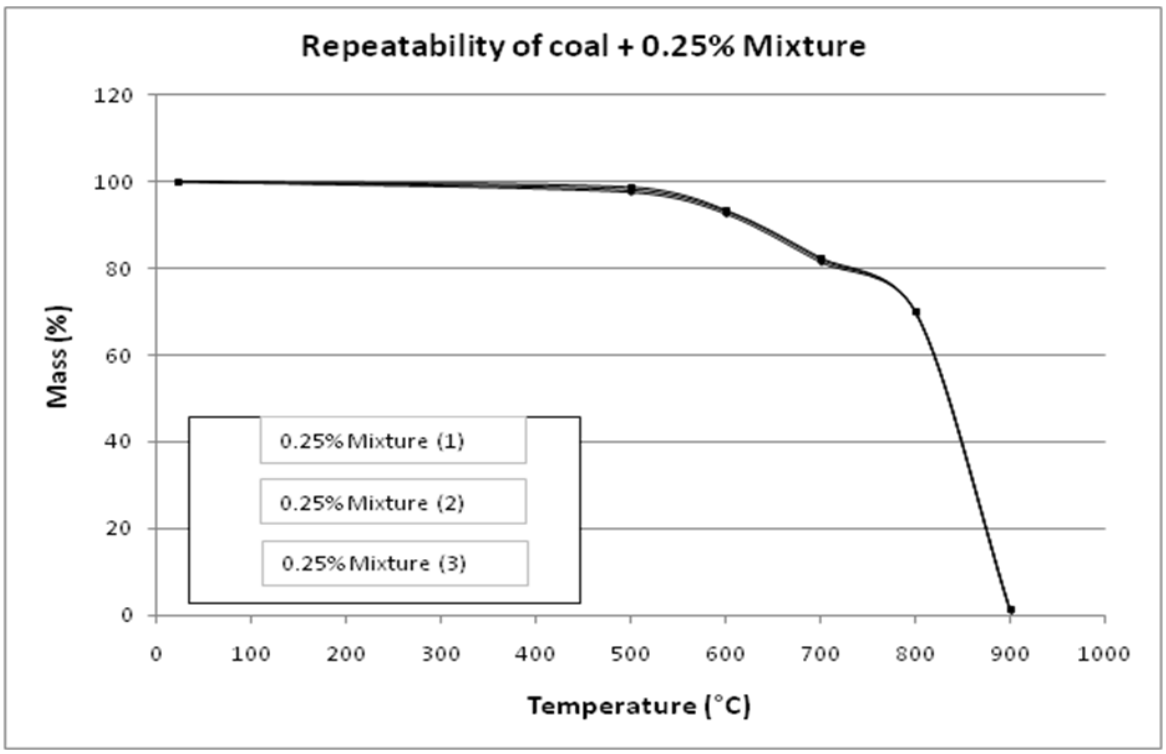

Figure 5.6: Repeatability of the mass loss of char from coal with pre-added 0.25% mixture of Na_2CO_3 and K_2CO_3 during thermal treatment under CO_2.

5.3.2 Coal with Catalyst Addition

Figure 5.7 summarizes the results obtained when the chosen catalysts were added to coal before charring and the chars were then subjected to the thermal treatment method as described in Section 4.4. The results shown in Figure 5.7 indicate that the demineralized char reached a total mass loss of 45% after 24 hours in the furnace under CO_2 atmosphere. Comparing the char mass loss to the catalyzed coal mass loss, it can be confirmed that potassium carbonate and sodium carbonate, as well as a mixture of the two, are good catalysts. The mass loss doubled for 0.25% to 4% pre-addition of potassium carbonate to char, increased approximately a third of the mass loss for 0.25% sodium carbonate pre-addition to char and doubled for 0.5% to 4% pre-addition. The mixture of the two catalysts also had a doubling effect on the mass loss in comparison to the mass loss observed for the reference sample (char without catalysts).

It is clear that the amount of catalyst mixture added to the coal (before charring) had little or no effect on the high conversion of close to a 100%, irrespective of addition concentration. It is possible that the mixture of the two catalysts forms a binary eutectic salt. The samples with a mixture of the catalysts had almost reached complete conversion after the same amount of time for all cases.

Complete conversion is almost reached for the char with added potassium and sodium carbonate thermal treatment CO_2 experiments, except for the 0.25% pre-additions of these two catalysts' addition. The maximum conversion was thus already observed after pre-addition of only 0.5% of the catalyst. It may be explained by the mechanism by which alkali metals influence the reactivity [Kapteijn et al., 1986] (See Section 2.5.1.1). The molten solutions of the catalysts are better catalysts, due to the fact that they are already more evenly distributed throughout the coal sample while being charred [Sheth et al., 2003]. Thus, lower temperatures can be used to obtain the same results, and/or thus faster CO_2 conversion (reactivity) occurs. This is clear when comparing the conversion of the char (fourth column in each set after the same time and conditions) (see Figure 5.7) i.e. doubling in reaction rate is achieved via catalyst pre-addition. During the gasification of the samples, the potassium carbonate and sodium carbonate transform to their oxides [Kapteijn et al., 1984]. This is confirmed by the QEMSCAN results in Section 5.6.

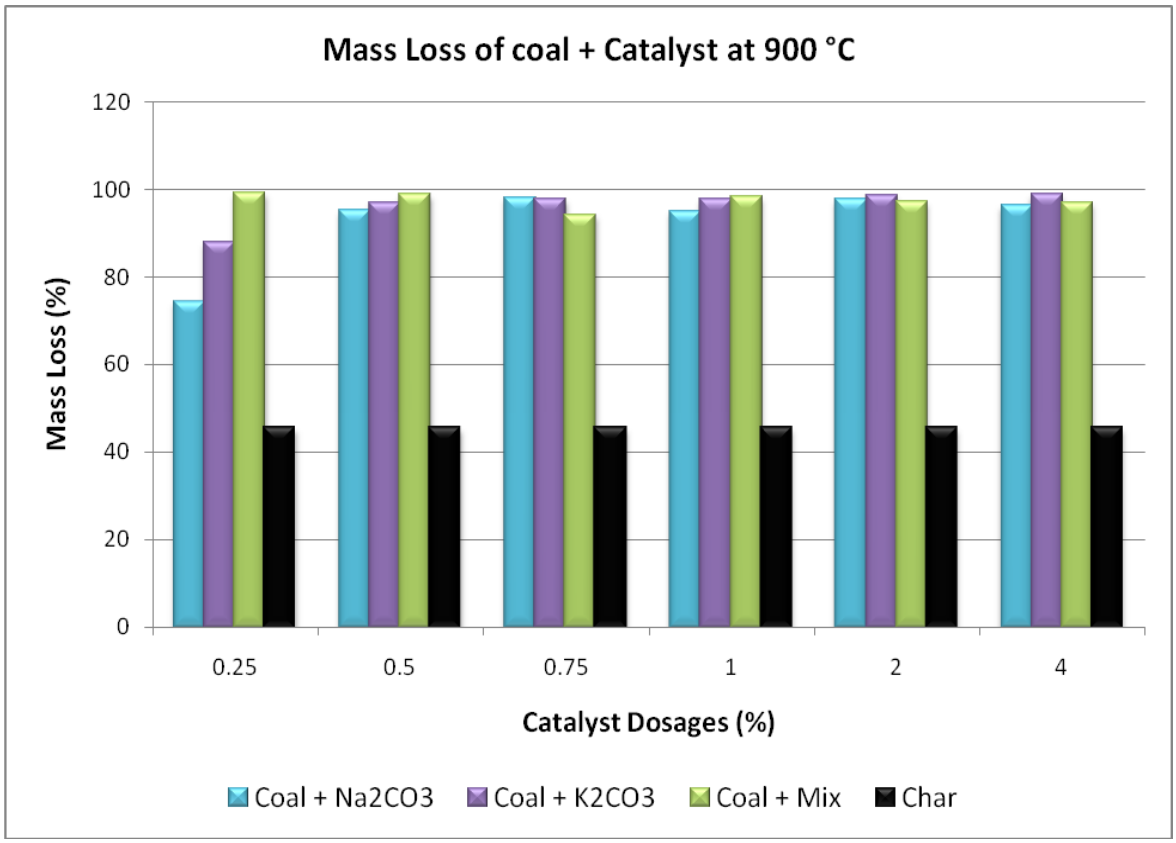

Figure 5.7: Schematic representation of mass loss of char from coal during charring with pre-added catalysts at 900 °C under CO_2.

5.3.3 Char with Catalyst Addition

Figure 5.8 summarizes the results obtained when the chosen catalysts were added directly to the chars and the chars were then subjected to the thermal treatment method as described in Section 4.4. When comparing Figure 5.8 to Figure 5.7, a definite influence is observed when adding catalyst before and after charring. The only two sets of data that almost correspond to each other are the 2% and 4% of K_2CO_3 additions and the mixture of the two catalysts additions. Binary eutectic salts form to a certain extent, but not completely [Sheth et al., 2003]. Potassium is a very mobile catalyst and together with the higher concentrations of catalyst the conversion increased [Nishiyama, 1991; Wood et al., 1984].

The sodium carbonate enriched char has a much lower conversion when post-added to char than when pre-added to coal and then charred, as seen when comparing Figures 5.7 and 5.8. The reason for this is that the molten solution of the catalyst, which has already formed an interface with the coal, can start to convert the coal at a much lower starting

temperature [Sheth et al., 2003; Takarada et al., 1986]. For the experiments performed and summarized in Figure 5.8 the catalyst still needs to decompose, melt and form an interface or layer on the coal (C-O-K/Na) [Suzuki et al., 1984; Takarada et al., 1986]. Thus, the catalytically induced part of the conversion of the coal starts at higher temperatures and at a later time, thereby limiting the conversion. Potassium carbonate at higher temperatures is very mobile and decomposes below gasification temperatures, as well as below the melting temperatures of the salt [Nishiyama, 1991; Wood et al., 1984; Moulijn et al., 1984]. The mobility of the potassium carbonate, its stronger association with carbonaceous substrates and its less volatile nature compared to sodium all contribute to potassium being a better catalyst than sodium [Kapteijn et al., 1986; Shadman et al.,1987; Nishiyama, 1991, Wood et al., 1984; Zhang et al., 2001]. Sodium exhibits less interaction with the carbon, and the consequence is that the carbonate is less easily distributed over the carbon [Kapteijn et al., 1986].

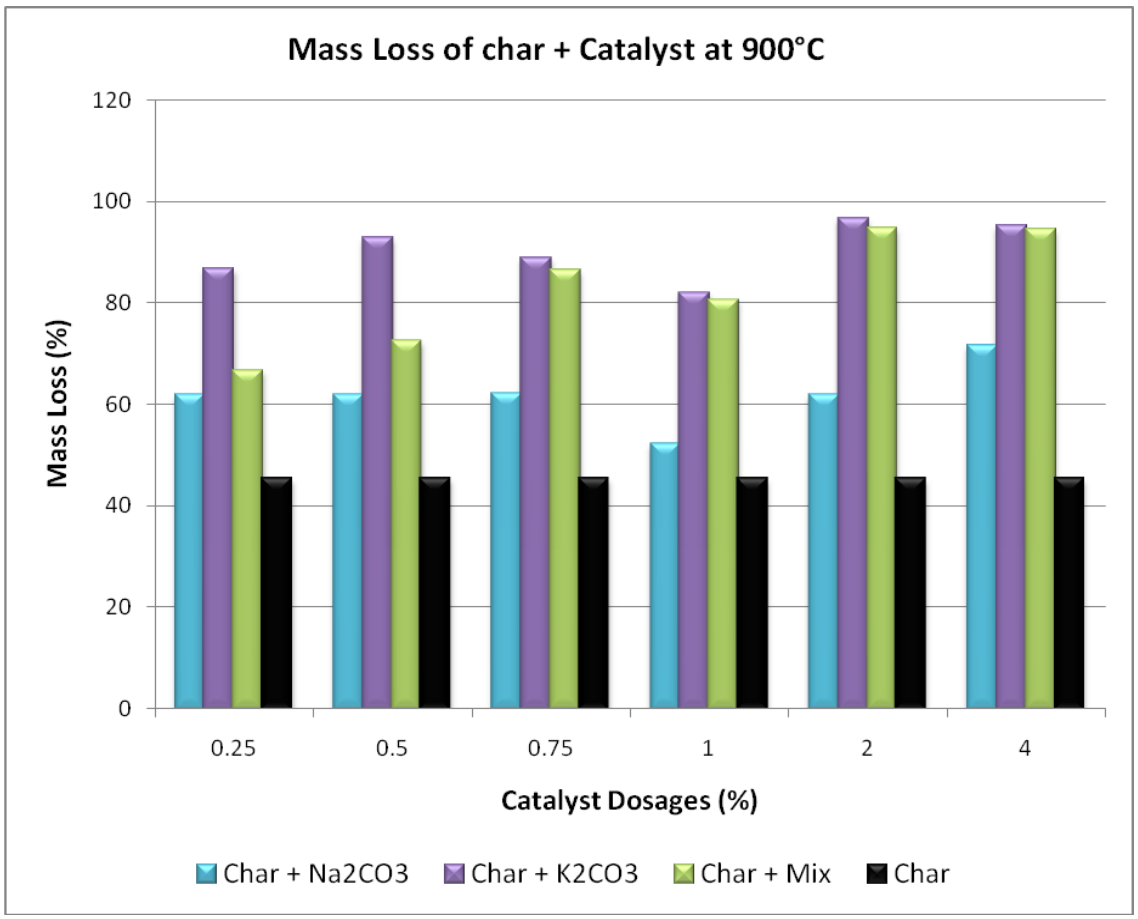

Figure 5.8: Schematic representation of mass loss of char with post-added catalysts at 900 °C under CO_2.

5.3.4 Comparison of Relative Reactivity of Pre- and Post added Catalysts to Char

Comparison of the two sets of samples; for example potassium carbonate, sodium carbonate and a mixture of the two catalysts pre-added to char and potassium carbonate, sodium carbonate and a mixture of the two catalysts post-added to char; is easily observed when placed in the same chart. In Figure 5.9 it is shown that there is a very large difference in mass loss when catalyst (Na_2CO_3) is added to the coal before charring and adding catalyst (Na_2CO_3) to the char. It is very clear that the decomposition of the carbonate and formation of the interface between the pre-added catalyst and the char before thermal treatment with CO_2 increase the conversion of the char dramatically in comparison with the other path followed. These results do not match the results found by Spiro et al. [1984]. A possible explanation for the difference in results is the particle size difference. Spiro et al. [1984] used larger particle sizes (500 µm), whereas the particle size in this study was -75 µm. This shows that only a small amount of catalyst is needed for catalytic conversion of char. Another reason for the difference in mass loss is the fact that the catalyst added to the char must still lose its volatiles, whereas when the catalyst is added to the coal prior to charring, the volatiles are already lost. The volatiles that are released together with the carbonates that decompose form a cloud around the sample and prevent the gas from reaching the char to gasify the sample immediately [Alvarez and Borrego, 2007].

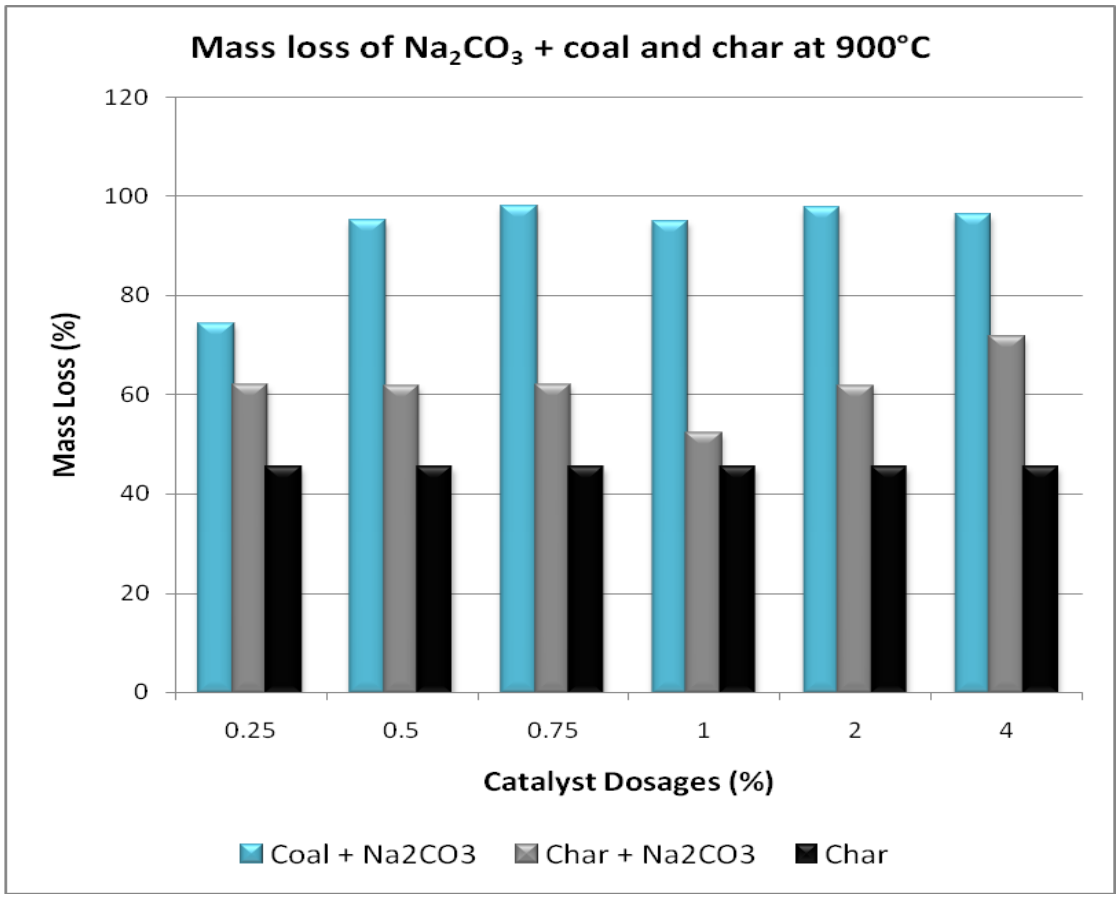

Figure 5.9: Schematic representation of mass loss of char with pre- and post added Na_2CO_3 at 900 °C under CO_2.

It can be observed in Figure 5.10 that the difference is much smaller for the samples with potassium carbonate as catalysts, possibly because potassium is a more mobile catalyst [Nishiyama, 1991; Wood et al., 1984]. Potassium thus is able to distribute itself faster and more efficient onto the surface of the char particles than sodium. There is a slightly lower conversion for the sample with catalyst added to the char than for the catalyst added to coal, but the difference is insignificant. The same conclusion was reached by Spiro et al. [1984]. In Figure 5.11 the same trend is seen as in Figure 5.10. There is almost complete conversion from the lowest addition of catalyst mixture.

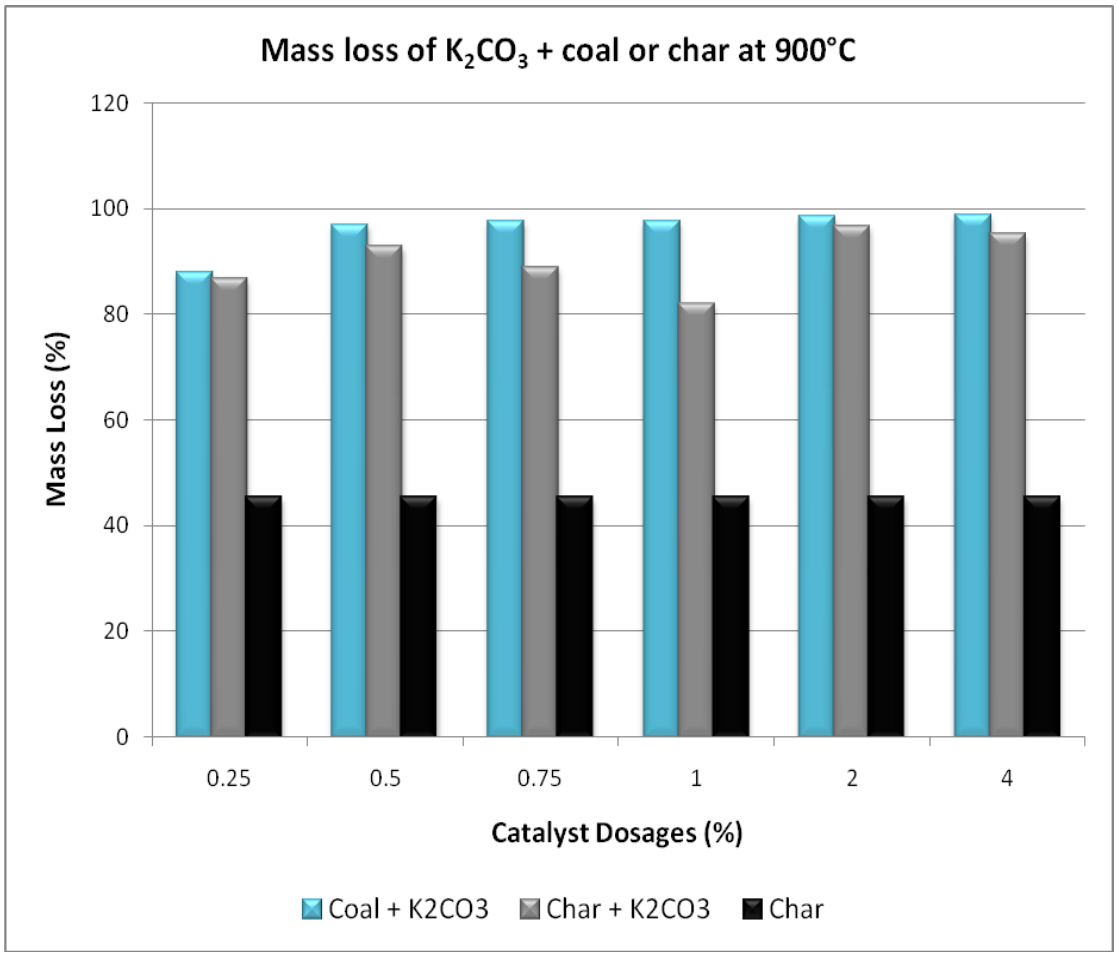

Figure 5.10: Schematic representation of mass loss of coal and char with added K_2CO_3 at 900 °C under CO_2.

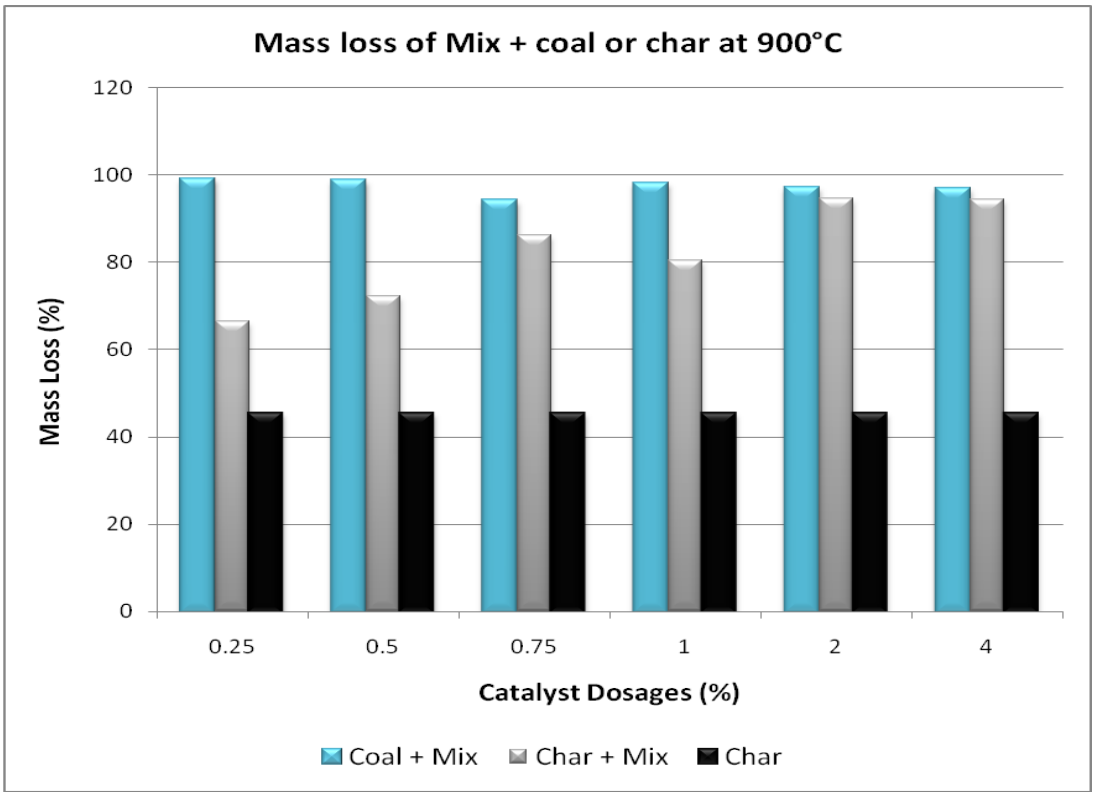

Figure 5.11: Schematic representation of mass loss of coal and char with added mixture of the two catalysts at 900 °C under CO_2.

This section described the effect of Na_2CO_3, K_2CO_3 and a mixture of the two added to coal and char on the total mass loss of the samples.

5.4 CO_2 BET Surface Area Determination

Table 5.3 shows the CO_2 BET surface area results of raw coal, demineralized coal, coal charred at 700 °C, coal with 4% addition of K_2CO_3 charred at 700 °C, coal charred at 900 °C and coal with 4% addition of K_2CO_3 charred at 900 °C. All the experiments were performed under analytical grade N_2.

It can be seen in Table 5.3 that the raw coal and the demineralized coal had approximately the same micropore surface areas. This can be explained by the collapsing of a small number of the micropores during the demineralization and drying process [Amarasekera et al., 1995]. In these micropores are water molecules that are closely associated with the coal. Coal has a high affinity for water and some of these molecules keep the micropores open [Amarasekera et al., 1995]. It is also known that microporosity increases during the charring of coal [Hamilton et al., 1984]. This is due to volatiles being

released from the coal during the process [Hamilton et al., 1984]. The slight decrease in microporosity from 700 °C to 900 °C may again be the collapsing of a small number of external or internal micropores. It is also proven that during gasification surface area initially increases and finally starts to decrease [Tseng and Edgar, 1989]. The addition of the catalyst before charring may help support some of the micropores from collapsing. Potassium is very mobile [Nishiyama, 1991; Wood et al., 1984] and will cover the surface of the micropores, preventing them from collapsing. There is not a notable change in the surface areas from 700 °C to 900 °C with the 4% wt. K_2CO_3 addition. The slight increase may have an effect on the reactivity of the char with and without added catalyst.

Table 5.3: Micropore surface area of raw coal, demineralized coal and demineralized coal char at two temperatures with and without 4% K_2CO_3.

Sample Name	Micropore Surface Area (m^2/g)
Raw Coal	147
Demineralized Coal	149
Char (700 °C)	440
Char (700 °C) + 4% K_2CO_3	447
Char (900 °C)	413
Char (900 °C) + 4% K_2CO_3	445

5.5 X-ray fluorescence and X-ray diffraction

Table 5.4 represents the X-ray fluorescence results of the catalysts used in the study to determine the purity. The results confirm that the catalysts were more than 99% pure and thus could not cause an increase in the concentrations of other elements in the products obtained during the various thermal studies. The X-ray fluorescence analyses performed on the different prepared samples are therefore due to the composition of the coal and char samples only with the exception of potassium and sodium. The results show that there is a very low sulphur and chlorine content (0.01% for K_2CO_3 and 0.02% for Na_2CO_3). It should be remembered for all the XRF results that the increase or decrease of any of the fractions only changes relative to the other fractions. It does not increase but the ratio does changes, which make the fraction seem larger.

Table 5.4: X-ray fluorescence results of K_2CO_3 and Na_2CO_3 to determine purity of the salts.

Sample	Fe_2O_3 (%)	MnO (%)	Cr_2O_3 (%)	V_2O_5 (%)	TiO_2 (%)	CaO (%)	K_2O (%)	P_2O_5 (%)	SiO_2 (%)	Al_2O_3 (%)	MgO (%)	Na (%)	Cl (%)	S (%)
K_2CO_3	0.01	0.05	0.01	0.01	0.01	0.02	99.34	0.01	0.1	0.01	0.01	0.4	0.01	0.01
Na_2CO_3	0.01	0.03	0.01	0.01	0.01	0.01	0.01	0.01	0.12	0.01	0.01	99.65	0.09	0.02

Table 5.5 represents the normalized data of demineralized char prepared at various temperatures (500 °C, 700 °C, 900° C) under nitrogen, as well as char prepared at 900 °C under nitrogen and then exposed to a CO_2 atmosphere. The largest fractions for all the samples are Fe_2O_3, (22.06% to 30.00%), CaO, (9.48% to 12.55%), and sulphur, (17.44% to 22.06%). The iron oxide increased with thermal treatment temperature, whereas the calcium oxide and the sulphur fractions decrease with thermal treatment temperature. The iron oxide reaches a maximum when gasified under CO_2 and calcium oxide and sulphur reaches a minimum under the same conditions. It should be remembered that the results for the sodium, chlorine and sulphur are semi-quantitative. These percentage changes are due to the fact that the carbonaceous parts of the samples react and are vaporized. The elemental compositions of the samples detected by XRF are reported as oxides by default.

Table 5.5: X-ray fluorescence results of demineralized, partly devolatilized coal at various temperatures under N_2 and finally CO_2.

Sample	Fe_2O_3 (%)	MnO (%)	Cr_2O_3 (%)	V_2O_5 (%)	TiO_2 (%)	CaO (%)	K_2O (%)	P_2O_5 (%)	SiO_2 (%)	Al_2O_3 (%)	MgO (%)	Na_2O (%)	Cl (%)	S (%)
PDC (500°C, N_2)	22.06	0.38	1.52	0.38	7.22	12.55	0.38	12.93	3.80	7.60	3.80	3.80	1.52	22.06
PDC (700°C, N_2)	28.01	0.35	1.77	0.35	7.80	11.71	0.35	9.58	3.55	7.09	3.55	3.55	1.42	20.92
PDC (900°C, N_2)	28.52	0.39	1.95	0.39	7.03	10.94	0.39	9.38	3.91	7.81	3.91	3.90	0.78	20.70
PDC (900°C, N_2, CO_2)	30.00	0.09	1.60	0.25	9.18	9.48	0.30	0.26	1.90	16.50	10.26	2.67	0.07	17.44

The potassium and sodium enriched char results in Table 5.6, confirmed that potassium salts are less volatile than sodium salts and stays captured in the ash of the char enriched samples [Muchmore et al., 1995; Sheldon et al., 1992]. The results indicate that the major portion of the alkali species was retained in the solid phase during gasification. When the coal with added potassium is charred at 500 °C under nitrogen, 42.18% of the remaining ash is potassium species. If the results are compared to the coal with added potassium charred and ashed at 900 °C under nitrogen and carbon dioxide, respectively,

42.92% is retained in the ash part. The increase may be due to inaccurate measurements. When observing the coal with added sodium sample's results charred at 900 °C under nitrogen, it can also be noticed that 47.71% was retained in the sample ash. It can be assumed that the largest part (>80%) of the potassium and sodium are captured in the ash [Muchmore et al., 1995; Sheldon et al., 1992]. Some crystalline forms of potassium chloride and potassium sulphate were observed from the X-ray diffraction results (Table 5.7). In this case, it seems that potassium has a high affinity for chlorine [Li et al., 2005], which is clearly seen for the XRF results in Table 5.6.

The chlorine fraction in the char is 1.52% and the fraction of chlorine with the addition of 4% potassium carbonate to coal is 7.71% at 500 °C under nitrogen; whereas the chlorine fraction for char treated under nitrogen and carbon dioxide at 900 °C is 0.07% and with added 4% potassium carbonate is 16.10%. There is thus a higher fraction of chlorine left as indicated by the results in Table 5.6. The same trend can be observed for the sodium results where the chlorine fraction is 16.10% when 4% Na_2CO_3 is added to the coal and thermally treated under nitrogen and then under carbon dioxide at 900 °C. The sulphur is mostly associated with the potassium and sodium as observed in the trend of the alkali metals and the sulphur. When the one fraction increases, the other increases [Punjak et al., 1989]. The X-ray diffraction results in Table 5.7 confirm this observation.

Table 5.6: X-ray fluorescence results of demineralized, partly devolatilized coal (PDC) with added K_2CO_3 and Na_2CO_3 under N_2 and finally CO_2.

Sample	Fe_2O_3 (%)	MnO (%)	Cr_2O_3 (%)	V_2O_5 (%)	TiO_2 (%)	CaO (%)	K_2O (%)	P_2O_5 (%)	SiO_2 (%)	Al_2O_3 (%)	MgO (%)	Na_2O (%)	Cl (%)	S (%)
PDC + 4% K_2CO_3 (500°C, N_2)	8.84	0.23	0.23	0.23	3.885	6.58	42.18	4.08	2.27	2.27	2.27	2.26	7.71	17.00
PDC + 4% K_2CO_3 (700°C, N_2)	13.99	0.16	1.54	0.16	4.27	6.66	43.86	2.90	1.71	1.71	1.71	1.70	12.29	7.34
PDC + 4% K_2CO_3 (900°C, N_2)	18.26	0.16	2.59	0.16	3.96	5.48	42.31	2.13	1.52	1.52	1.52	1.52	12.02	6.85
PDC + 4% K_2CO_3 (900°C, N_2, CO_2)	10.57	0.03	0.50	0.08	2.90	2.67	42.92	0.08	1.42	4.10	1.06	1.06	13.71	17.59
PDC + 4% Na_2CO_3 (900°C, N_2)	3.98	0.19	0.60	0.08	5.77	2.78	0.60	0.40	1.99	5.96	2.58	47.71	16.10	10.54

Table 5.7: X-ray diffraction results of partly devolatilized coal with added potassium carbonate treated under nitrogen and carbon dioxide.

PDC + 4% K_2CO_3 (900 °C, N_2, CO_2)	Mineral
	Sylvite (KCl)
	Potassium Sulphate (K_2SO_4)
	Iron Oxide (Fe_2O_3)

Table 5.8 is a modified normalized version of Table 5.6, where the fractions of potassium and sodium were lowered to the original amounts before catalyst addition. This was done to determine the actual change in the fractions of specific species in the ash, such as iron oxide, chlorine and sulphur. When Table 5.8 is compared to Table 5.6 the iron content only changes for the first and fourth potassium addition samples. The reason for this being that potassium forms low melting species with iron moieties [Punjak et al., 1989]; whereas for the fourth potassium addition samples the potassium is probably more closely associated with the chlorine than with the iron. The iron oxide fraction in the sodium treated coal is much lower, which indicates that the sodium is not as closely associated with the iron as potassium.

Calcium oxide undergoes a small change in the potassium treated samples (from 11.33% to 12.55%), except for the fourth potassium treated sample where the calcium oxide is approximately half the fraction with added potassium than without potassium. The largest change for the potassium and sodium treated coal occurs for the chlorine fraction. Chlorine is present in a higher than expected fraction for the leached coal because of chlorides being caught in the structure during demineralization procedure where hydrochloric acid was used. Extensive washing with demineralized water could not get rid of these chloride species. As previously mentioned, alkali metals have a high affinity to halogens and thus chlorine associates with the potassium and sodium species and does not volatilize to a large extent [Li et al., 2005]. The chlorine is present as KCl in the potassium treated coal. The sulphur fraction is not affected by the sodium addition. For the potassium treated coal the sulphur fraction increases, but to a much smaller extent than the chlorine. Sulphur is also associated with the potassium as K_2SO_4 as seen from the X-ray diffraction results presented in Table 5.7. This is also retained in the ash in the crystalline form together with KCl. These results were also found in the QEMSCAN results in Section 5.6.

Table 5.8: Modified X-ray fluorescence results of Table 5.6.

Sample	Fe_2O_3 (%)	MnO (%)	Cr_2O_3 (%)	V_2O_5 (%)	TiO_2 (%)	CaO (%)	K_2O (%)	P_2O_5 (%)	SiO_2 (%)	Al_2O_3 (%)	MgO (%)	Na_2O (%)	Cl (%)	S (%)
PDC + 4% K_2CO_3 (500°C, N_2)	15.23	0.39	0.39	0.39	6.64	11.33	0.39	7.03	3.91	3.91	3.91	3.90	13.28	29.30
PDC + 4% K_2CO_3 (700°C, N_2)	24.85	0.30	2.73	0.30	7.58	11.82	0.30	5.15	3.03	3.03	3.03	3.02	21.82	13.03
PDC + 4% K_2CO_3 (900°C, N_2)	31.58	0.26	4.47	0.26	6.84	9.47	0.26	3.68	2.63	2.63	2.63	2.62	20.79	11.84
PDC + 4% K_2CO_3 (900°C, N_2, CO_2)	18.38	0.05	0.88	0.14	5.05	4.64	0.74	0.14	2.47	7.13	4.12	1.84	23.84	30.59
PDC + 4% Na_2CO_3 (900°C, N_2)	7.33	0.37	1.10	1.47	10.62	5.13	1.10	0.73	3.66	10.99	4.76	3.66	29.67	19.41

5.6 QEMSCAN

QEMSCAN analyses were performed on the following samples; char, pre-added 4% potassium carbonate and 4% sodium carbonate to char, prepared ash from pre-added potassium carbonate to char and the separate catalysts. The density of the char was determined to be 1.8 g/cm^3. The assumed density of Na_2CO_3 (nitrite) is 2.54 g/cm^3 and for K_2CO_3 is 2.29 g/cm^3 [TPTCLOU, 2011a; TPTCLOU, 2011b]. Based on this assumption the calculated ash content of the demineralized coal is 1.2% and the total mineral matter content is 1.7%.

From Table 5.9 it can be seen that the major mineral present in the demineralized char is pyrrhotite ($Fe_{0.95}S$) with a value of 1.24%. For the chars with pre-added potassium and sodium carbonate, pyrrhotite exceeds 1% as can be observed from Table 5.9. The char sample with pre-added potassium carbonate has the highest pyrrhotite level present (1.41%), which supports the literature that potassium has a higher affinity to sulphur compared to sodium [Spiro et al., 1986]. This corresponds well with the results of the XRF analysis performed on the same char as described in Table 5.5. The iron and sulphur fractions are 28.52% and 20.70% respectively, thus the ratio of these two elements supports that pyrrhotite will be the favoured composition. Pyrrhotite is the partial high temperature transformation phase of pyrite (FeS_2). Extraneous particles or coarse included grains were the predominant forms pyrrhotite occurs. In Figure 5.12 shows is a sample of pyrrhotite

present in the char. The sulphur is presented as yellow fractions and sulphur-poor fractions are grey.

There are trace (<0.1 mass%) proportions of included kaolinite, quartz and rutile in the demineralized char, char with pre-added potassium carbonate and char with pre-added sodium carbonate as seen in Table 5.9.

Table 5.9: Mineral proportions of the demineralized char with added K_2CO_3 and Na_2CO_3 respectively.

Mineral	Composition	Char (%)	A*(%)	B**(%)
Sulphates/Gibbsite	Ca- and Al-bearing sulphates	0.02	0.04	0.03
Pyrrhotite	$Fe_{0.95}S$	1.24	1.41	1.21
Magnetite/Siderite	$Fe_3O_4/FeCO_3$	0.00	0.02	0.00
Calcite	$CaCO_3$	0.00	0.00	0.00
Dolomite	$CaMg(CO_3)_2$	0.00	0.00	0.00
Apatite	$Ca_5(PO_4)_3(OH,F,Cl)$	0.01	0.01	0.00
Kaolinite	$Al_2Si_2O_5(OH)_4$ (clay)	0.08	0.02	0.01
Quartz	SiO_2 (sand)	0.08	0.68	0.06
Illite/Hydro-Muscovite	$K_2Al_6Si_6O_{20}(OH)_4$/ $KAl_5Si_7O_{20}(OH)_4$	0.01	0.04	0.01
Albite/Microcline	$(K,Na)AlSi_3O_8$	0.00	0.02	0.00
Rutile	TiO_2	0.05	0.10	0.06
Char-organic S bearing ("Bright Coal")	C,H,O,N,S	53.23	41.58	49.27
Char ("Dull Coal")	C,H,O,N	45.13	46.96	40.91
K_2CO_3/Na_2CO_3	Catalyst added	0.15	9.13	8.44
Total		**100.00**	**100.00**	**100.00**
Mineral Matter/Ash reconciliation				
Total Mineral Matter	100-Total ("Coal")	1.65		
Mineral-derived volatiles	Calculated	0.48		
QS Calculated Ash-%	MM-MV	1.17		

*Char with pre-added 4% K_2CO_3, charred under N_2 atmosphere.

**Char with pre-added 4% Na_2CO_3, charred under N_2 atmosphere.

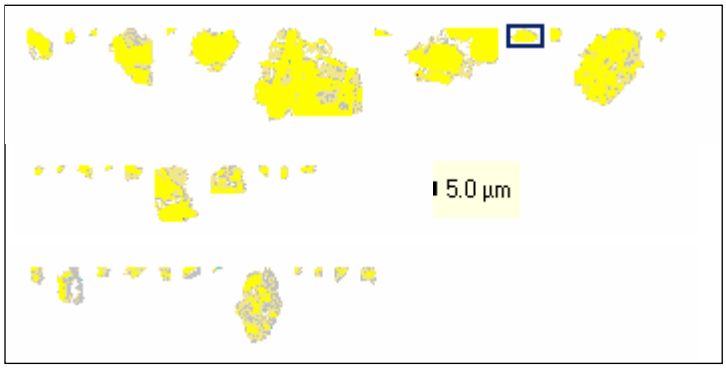

Figure 5.12: A few samples of pyrrhotite (yellow) rich particles in demineralized char. Sulphur-rich is dark yellow, whereas sulphur-poor char is grey. Scale bar is 5 microns.

Na_2CO_3 and K_2CO_3 in the demineralized char samples occurred as extraneous spherical particles as seen in Figures 5.13 and 5.14. The catalysts pre-added to the char transformed into either a potassium oxide or sodium oxide. It is confirmed in literature by Kapteijn et al. [1984], Takarada et al. [1986], Kühn and Plogmann [1983], and Chen and Yang [1997]. The majority of sodium and potassium in these samples occur as the high temperature transformed product of the original catalyst. Some of the Na_2CO_3 and K_2CO_3 catalyst in the char samples have absorbed chlorine to form either sylvite (KCl) or halite (NaCl) as observed in Figures 5.13 and 5.14. This is due to the fact that alkali metals have a high affinity to halogens [Li et al., 2005]. In Figure 5.13 sodium oxide particles are blue whereas NaCl are depicted as black. In Figure 5.14 potassium carbonate are seen as dark blue and potassium carbonate is black. It is clear that the oxides of the alkali metals predominate.

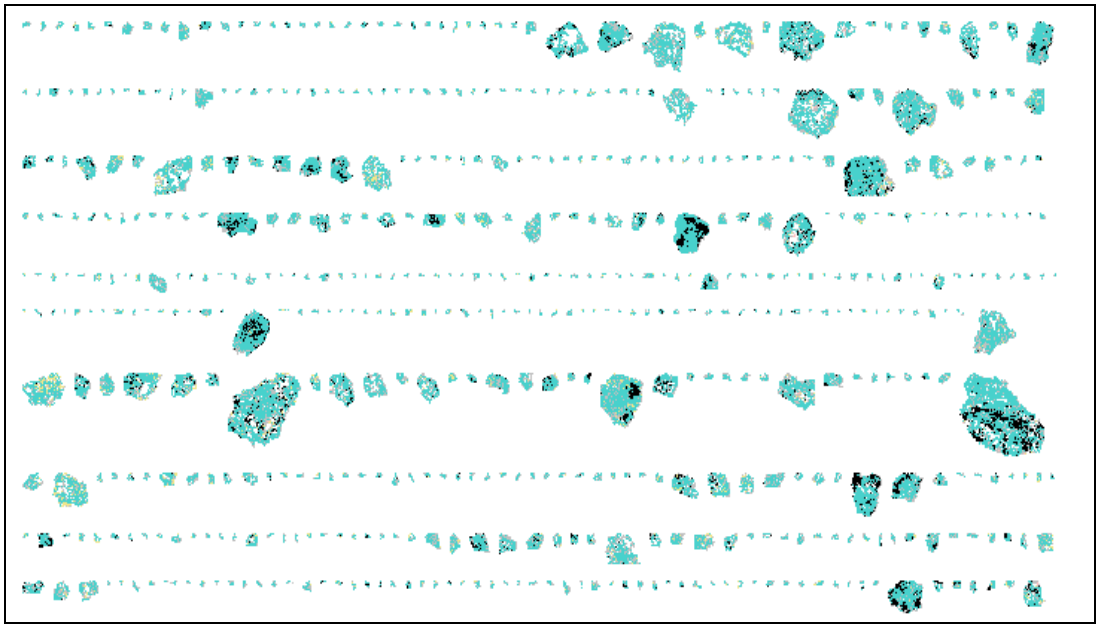

Figure 5.13: Na-oxide particles (blue) in the demineralized char with pre-added 4% Na_2CO_3 sample. NaCl is black.

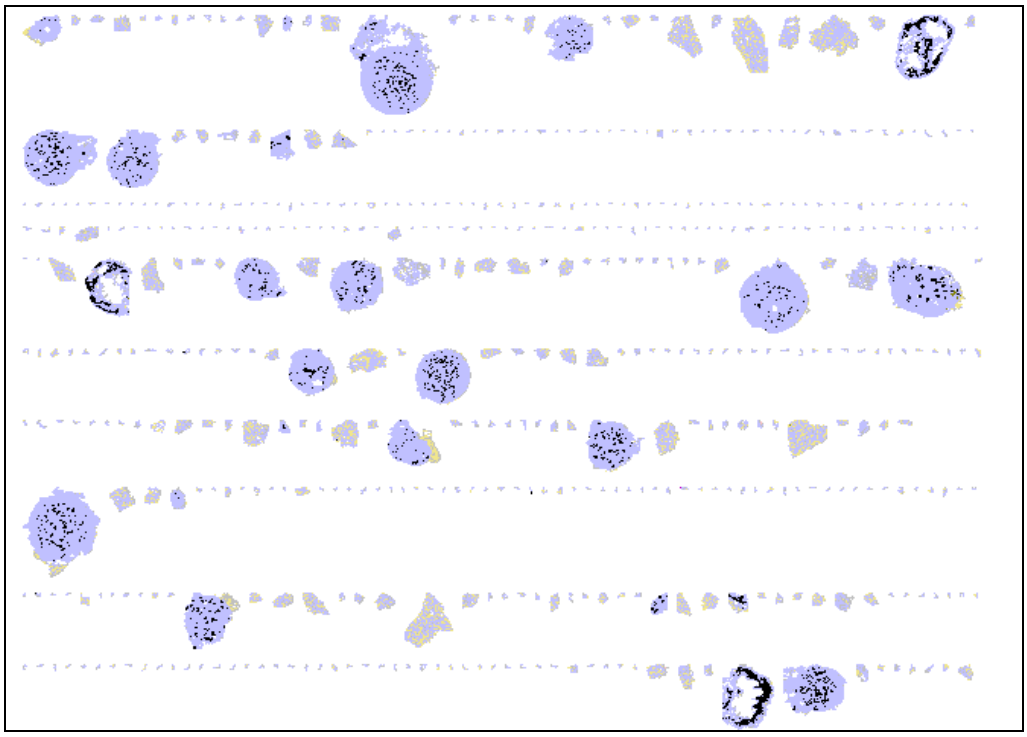

Figure 5.14: K-oxide particles (dark blue) in the demineralized char with pre-added 4% K_2CO_3 sample. KCl is black.

During the analysis there was no KCl or NaCl found in the raw catalyst samples, but KCl and NaCl was present in the demineralized catalyzed charred samples. It can thus be assumed that Cl is derived either from the coal/char or was introduced during the process of charring. The XRF results of the char in Table 5.5 indicate a low content of chlorine present (0.07%). Thus it can be concluded that the chlorine was introduced into the system via the demineralization process. During observation of Figure 5.15, it was noticed that potassium sulphate laths are a common constituent in char with pre-added 4% K_2CO_3 ash sample. Organically bound sulphur in the char and sulphur derived from pyrite/pyrrhotite has possibly reacted with potassium to form these potassium sulphate laths.

Potassium-rich aluminosilicate and potassium silicate with trace to minor concentrations of iron, calcium and magnesium is the other main potassium bearing phase in the char with pre-added 4% K_2CO_3 sample. Potassium rich aluminosilicate are the dominant phase in the char with pre-added 4% K_2CO_3 ash. These phases can contain trace to minor concentrations of fluxing elements (Fe, Ca and Mg). These fluxing elements (Fe, Ca and Mg) are the possible cause for the inability to prepare ash from Na_2CO_3 for further analysis. During the thermal treatment of the mixture of sodium carbonate and demineralized coal, sodium oxide reacted with chloride and sulphate from the organically-bound sulphur and pyrite to form sodium chloride and sodium sulphate respectively. The formed sodium chloride reacted with sodium sulphate at 627°C to form a melt [Wood and Breithaupt, 1952]. Potassium sulphate is present in the char with pre-added 4% K_2CO_3 ash sample.

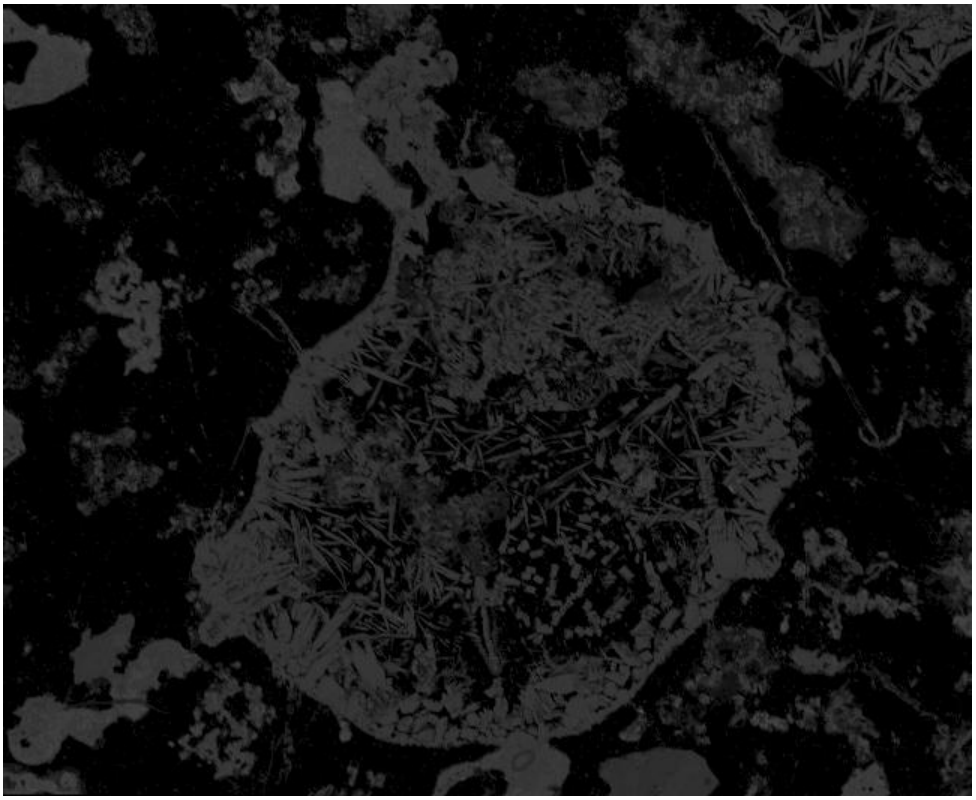

Figure 5.15: Distinct potassium sulphate crystals (light grey area) in char with pre-added 4% K_2CO_3 sample ash.

Chapter 6

Conclusions

In this chapter, the general conclusions derived from this research are given. The extent to which the aims and objectives of this study were reached and are mentioned in this section. Recommendations based on the results of this investigation are also given, which can give direction to future studies.

6.1 Ash Percentage Determination and Proximate Analysis

A South African coal was demineralized optimally and submitted for proximate analysis. The ash percentage analysis and proximate analysis results proved that the demineralization procedure was successful in removing the effect of the some mineral matter. The raw coal had an ash content of 26.2% and the demineralized coal had an ash content of 1.8%.

6.2 Ultimate Analysis and Ash Fusion Temperature Tests

When the ultimate analysis results are studied, no noticeable change in the two samples (raw and demineralized coal) was observed. It can thus be concluded that the demineralization process does not greatly affect the macromolecular composition of the coal. The lowered ash fusion temperature suggested the removal of aluminosilicates during the demineralization procedure. Sodium carbonate formed a liquid melting phase with the coal sample and no ash could be obtained to measure ash fusion temperatures or QEMSCAN results.

6.3 CO_2 Thermal Treatment

To determine relative reactivity of the catalyzed and untreated char samples, a new method was developed. This method (as described in Chapter 4) can be deemed successful when observing the repeatability results, which showed a standard deviation of less than

3%. Catalysts were pre- and post-added to demineralized char (0.25%, 0.5%, 0.75%, 1%, 2% and 4%) and thermally treated in the furnace from 500 °C to 900 °C under CO_2. The catalysts were potassium carbonate, sodium carbonate and a 1:1 mixture of the two catalysts.

Table 6.1: Summarized data of the total mass loss of the coal and char samples with catalyst additions at 900 °C under CO_2.

	Catalyst Addition Concentration					
Sample	**0.25%**	**0.5%**	**0.75%**	**1%**	**2%**	**4%**
Char*	45.2	45.2	45.2	45.2	45.2	45.2
Pre-added Na_2CO_3	74.1	94.8	97.8	94.7	97.4	96.0
Pre-added K_2CO_3	87.6	96.7	97.4	97.4	98.3	98.5
Pre-added Mixture	98.9	98.5	93.9	97.9	96.9	96.7
Post-added Na_2CO_3	61.7	61.6	61.8	52.0	61.6	71.4
Post-added K_2CO_3	86.5	92.6	88.7	81.8	96.5	94.9
Post-added Mixture	66.5	72.3	86.2	80.4	94.6	94.3

*Char = Sample with no catalyst addition. Included for comparative reasons.

6.3.1 Coal with Catalyst Addition

Untreated char showed a low conversion rate of 45% after 24 hours in the furnace at 900 °C under a CO_2 atmosphere. When observing Table 6.1 it can be seen that pre-addition of catalyst to the coal before charring, results in the char having a high conversion rate for Na_2CO_3, K_2CO_3 and the mixture from 0.5% addition to coal before charring. Thus it could be concluded that adding catalysts to coal char has a positive effect on relative reactivity with a mass loss of more than 95%. The high mass loss is an indication of the very high CO_2 conversion of this char.

6.3.2 Char with Catalyst Addition

When observing Table 6.1 it can be seen that only K_2CO_3 enriched char shows a high conversion rate from lower additions of catalyst up to 4% pre-addition of catalyst. Na_2CO_3 enriched char shows low conversion irrespective of the Na_2CO_3 concentration. The highest conversion for Na_2CO_3 enriched char is approximately 70%. The mixture of the catalysts had

a low conversion rate at lower concentrations, but from a 0.75% concentration the Na_2CO_3 results follow the same trend as K_2CO_3 addition to char. The highest conversion is approximately 95%.

6.3.3 Comparison of Pre- and Post-Addition of Catalysts to Char

When observing Table 6.1, it can noted that Na_2CO_3 pre-addition of catalyst to char shows much better conversion rates, than for post-addition of Na_2CO_3. For K_2CO_3 as added catalyst the change is much smaller and it can be accepted that pre- and post-addition for this catalyst hardly had an effect. When observing Table 6.1 it was observed that pre-addition of the mixture of the catalysts shows a large conversion from the lowest concentration, whereas the conversion increases with the increasing amounts of post-added catalyst mixture.

6.3.4 Conclusion of Thermal Treatment

K_2CO_3 enriched char has the highest reactivity irrespective of the concentration of the catalyst. It also has no influence whether K_2CO_3 is pre- or post-added to char.

Na_2CO_3 enriched char has the lowest reactivity of the two added catalysts, but pre-addition increases the reactivity in such a way that it equals K_2CO_3 addition and the mixture of the catalysts' results.

Addition of a mixture of the two studied catalysts has the same reactivity as the char with pre-added K_2CO_3 and resembles the reactivity of the char with post-added Na_2CO_3. Nearly a complete CO_2 conversion was observed from 2% addition of the catalysts.

6.4 CO_2 BET Surface Area Determination

Table 5.3 shows the micropore surface area of various coal and char samples. The surface area of the coal and demineralized coal is similar although collapsing of pores during the demineralization and drying process may result in a small increase. Surface area increases with charring of coal and during catalyst addition as the pores are structurally supported by the catalysts and tend to stay open. The support of the micropores also helps with the increase in reactivity.

6.5 XRF and XRD Results

XRF results of the catalysts showed that the catalysts contained very few impurities such as chlorine, sulphur and iron.

XRF results of demineralized char at various temperatures showed fractions of elements (as their respective oxides) present in the demineralized char.

Table 5.6 represents the XRF results of the char with pre-added potassium and sodium carbonates to char. It can be observed from these results that potassium and sodium species were retained in the ash in large fractions. The Cl and S fractions also remain higher than in the untreated char samples. This is supported by the XRD results in Table 5.7.

Table 5.8 is a modified set of XRF results. This shows that the relative amounts of chlorine and sulphur increase as the temperature increase especially under the CO_2 atmosphere for both K_2CO_3 and Na_2CO_3 additions. The last observation indicates that the chlorine and sulphur mostly remain in the coal char ash.

6.6 QEMSCAN

Potassium carbonate and sodium carbonate catalysts have transformed into potassium and sodium oxides. Sylvite (KCl) and halite (NaCl) are the respective salts that formed due to the fact that chlorine, either derived from the coal or added to the system, has reacted with the Na_2CO_3 and K_2CO_3 catalysts (possibly their oxide forms). Sodium-, potassium-oxide, NaCl and KCl are the major sodium- and potassium-bearing mineral phases in the char samples. In the pre-added 4% K_2CO_3 and pre-added Na_2CO_3 char samples there were no other major potassium- and sodium bearing minerals present. Only in the ash derived from pre-added 4% K_2CO_3 char sample potassium sulphate was present. Potassium sulphate could have been formed during the reaction of potassium with organically bound sulphur and pyritic sulphur. In the prepared ash sample, potassium aluminosilicate and potassium silicate is the other major ash present.

6.7 Objectives and Aims Achieved

1. *Demineralizing coal to remove the effect of the inherent minerals in coal for reactivity measurements and analytical experiments.*

   It was deemed a successful process, due to the fact that 93% of the ash content/yield were removed. It can also be supported by the lower ash content of 1.8% from 26%.

2. *Develop a method to determine relative CO_2 reactivity.*

   The development of the method was successful, due to the fact that the variance the results obtained through the thermal treatment method (Section 4.4) was less than 3%.

3. *Adding different amounts of catalyst and a mixture of catalysts before and after charring to determine the effects it has on CO_2 reactivity of the coal char.*

   The effects were successfully determined using the new developed reactivity measurement method. The reactivity has been increased in both cases of the singular catalyst additions and the mixture of the two catalysts. The results were discussed in detail in Chapter 5.

4. *Focus on the influence of potassium and sodium carbonate additions (as well as a mixture of the two) to evaluate the catalytic effect of the formed potassium and sodium species.*

   In Chapter 2 proposed mechanisms in literature give the possible catalyst species formed during catalytic gasification. QEMSCAN analysis also determined the species formed after charring and ashing of the char samples.

5. *Using different analytical techniques to determine the forms of potassium and sodium species after thermal treatments and addition before and after charring.*

   Two analytical techniques were employed to determine the species, i.e. XRD and QEMSCAN. Potassium species present in the char sample after pre-addition and potassium species present in the ash were determined. Sodium carbonate added to

the coal (before charring) was determined using QEMSCAN, but no ash could be prepared due to the fluxing qualities of sodium.

6. *Determining the optimum amount of catalyst addition.*
   The optimum amount of catalyst has been determined for potassium carbonate, sodium carbonate and the mixture of the two catalysts. It is described in the schematic representations in Chapter 5.

7. *Evaluating if there is a difference in adding the potassium and sodium carbonate before and after charring of the coal.*
   A difference was observed for sodium carbonate and the mixture of the two catalysts, but not for potassium carbonate added to either coal or char.

8. *To determine which species of potassium and sodium remain in the ash.*
   QEMSCAN and XRD analysis were performed to obtain these results, but could not be obtained for Na_2CO_3 and the mixture of the two catalysts due to the fluxing nature of the catalysts. Why sodium sulphate was not detected by QEMSCAN in the ash from PDC + sodium carbonate is because the formed sodium chloride reacted with sodium sulphate at 627 °C to form a melt (amorphous material). The remaining potassium species were identified.

6.8 Recommendations and Future Studies

The relative reactivity of small additions of K_2CO_3 added to coal can be determined to compare the results to the catalyst addition to char. It can be determined by the experiments if the CO_2 reactivity will increase. The addition of small amounts of K_2CO_3 to coal, if it does increase the CO_2 reactivity, can possibly hold industrial advantages such as increasing the gasification rate. Catalyst additions below 0.25% could be investigated as well. Future studies include the investigation of the kinetics of the various reactions to determine the activation energies for the various processes. The kinetics would give a better description of the influence of these compounds. Unfortunately K_2CO_3 can react with meta-kaolinite ($Al_2O_3.2SiO_2$) at elevated temperatures of greater than 1000 °C to big clinkers/agglomerates ($KAlSi_3O_8$).

References

Adánez, J., Miranda, J.L., Gavilán, J.M., 1985. Kinetics of a lignite-char gasification by CO_2. Fuel 64, 801-804.

Alvarez, D., Borrego, A.G., 2007. The evolution of char surface area along pulverized coal combustion. Energy and Fuels 21, 1085-1091.

Amarasekera, G., Scarlett, M.J., Mainwaring, D.E., 1995. Micropore size distributions and specific interactions in coals. Fuel 74, 115-118.

American Society for Testing and Materials. ASTM D4239-10e1:2010. Standard test methods for sulphur in the analysis sample of coal and coke using high-temperature tube furnace combustion methods. ASTM International.

American Society for Testing and Materials. ASTM D5373:2008. Standard test methods for instrumental determination of carbon, hydrogen, and nitrogen in laboratory samples of coal. ASTM International.

Audley, G.J., 1987. An evaluation of methods for enhancing the CO_2-reactivity of a caking bituminous coal. Fuel 66, 1635-1641.

Barroso, J., Ballester, J., Ferrer, L.M., Jiménez, S., 2006. Study of coal ash decomposition in an entrained flow reactor: Influence of coal type, blend composition and operating conditions. Fuel Processing Technology 87, 737-752.

Bauer, H.H., Christian, G.D., O'Reilly, J.E., 1978. Instrumental analysis: Techniques and applications. Dordrecht : Kluwer Academic Publishers. 264 p.

Bend, S.L., 1992. The origin, formation and petrographic composition of coal. Fuel 71, 851-870.

Brunauer, S., Emmett, P.H., Teller, E., 1938. Adsorption of gases in multimolecular layers. J. Chem. Soc. 60, 309-319.

Cairncross, B., 2001. An overview of the Permian (Karoo) coal deposits of Southern Africa. African Earth Sciences 33, 529-562.

Calo, J.M., Zhang, L. 1995. Characterization of porosity via secondary reactions. Quarterly Technical Report, Rhode Island. 19 p.

Chen, S.G., Yang, R.T., 1997. Unified mechanism of alkali and alkaline earth catalyzed gasification reactions of carbon by CO_2 and H_2O. Energy and Fuels 11, 421-427.

Choudhury, N., Chaudhuri, S.G., Chakraborty, C.C., Boral, P., 2004. Studies on char morphology in relation to petrographic characteristics of some Permian coals of India. Indian Journal of Scientific & Industrial Research 63, 383-385.

Clarkson, C.R., Bustin, R.M., 1996. Variation in micropore capacity and size distribution with composition in bituminous coal of the Western Canadian Sedimentary Basin. Implications for coalbed methane potential. Fuel 75, 1483-1498.

Cody, G.D., Davis, A., Hatcher, P.G., 1993. The dynamic nature of coal's macromolecular structure: Viscoelastic analysis of solvent-swollen coals. Energy & Fuels 7, 463-468.

Creelman, R.A., Ward, C.R., 1996. A scanning electron microscope method for automated, quantitative analysis of mineral matter in coal. Int. J. Coal Geol. 30, 249-269.

Crelling, J.C., 2009. Coal Characterization Research Program. [Web:] http://mccoy.lib.siu.edu [Date of use: 25 June 2010].

Cullity, B.D., 1959. Elements of X-ray diffraction. Massachusetts : Addison-Wesley Publishing Company, Inc. 514 p.

Davidsson, K.O., Korsgren, J.G., Pettersson, J.B.C., Jäglid, U., 2002a. The effects of fuels washing techniques on alkali release from biomass. Fuel 81, 137-142.

Davidsson, K.O., Stokjova, B.J., Pettersson, J.B.C., 2002b. Alkali emission from Birchwood particles during rapid pyrolysis. Energy and Fuels 16, 1033-1039.

Dayton, D.C., Jenkins, B.M., Turn, S.Q., Bakker, R.R., Williams, R.B., Belle-Oudry, D., Hill, L.M., 1999. Release of inorganic constituents from leached biomass during thermal conversion. Energy & Fuels 13, 860-870.

Donahue, C.J., Rais, E.A., 2009. Proximate analysis of coal. Journal of Chemical Education 86, 222-224.

Dutta, S., Wen, C.V., Belt, R.J., 1977. Reactivity of coal and char. 1. In carbon dioxide atmosphere. Ind. Eng. Chem., Process Des. Dev. 16, 20-30.

Dzubay, T.G., 1978. X-ray fluorescence analysis of environmental samples. Michigan : Ann Arbor Science Publishers. 310 p.

Galbreath, K., Zygarlicke, C., Casuccio, G., Moore, T., Gottlieb, P., Agron-Olshima, N., Huffman, G., Shah, A., Yang, N., Vleeskens, J., Hamburg, G., 1996. Collaborative study of quantitative coal mineral analysis using computer-controlled scanning electron microscopy. Fuel 75(4), 424-430.

Gasification Technologies Council (GTC), 2008. Gasification – Refining Clean Energy. [Web:] www.gasification.org [Date of use: 11 June 2010].

Goblirsch, G.M., Benson, S.A., Karner, F.R., Rindt, D.K., Hajicek, D.R. 1984. AFBC bed material performance with low-rank coals. Twelfth Biennial Lignite Symposium: Technology and Utilization of Low-Rank Coal Proceedings 2, 557.

Gottwald, U., Monkhouse, P., Wulgaris, N., Bonn, B., 2002. In-situ study of the effect of operating conditions and additives on alkali emissions in fluidized bed combustion. Fuel Processing Technology 75, 215-226.

Grigore, M., Sakurovs, R., French, D., Sahajwalla, V., 2008. Mineral matter in coals and their reactions during coking. Int. J. Coal Geol. 76, 301-308.

Günzler, H., Williams, A., 2002. Handbook of analytical techniques. Weinheim : Wiley-VCH. 1182 p.

Gupta, R., 2007. Advanced coal characterization: A review. Energy Fuels 21, 451-460.

Guthrie, J.M., 2010. Overview of x-ray fluorescence. [Web:] http://archaeometry.missouri.edu/xrf_overview.html [Date of use: 30 December 2010].

Hamilton, R.T., Sams, D.A., Shadman, F., 1984. Variation of rate during potassium-catalyzed CO_2 gasification of coal char. Fuel 63, 1008-1012.

Harrison, J.A., 1959. Effect of high-carbon components and other additives upon character of cokes: Laboratory scale study. Division of Gas and Fuel Chemistry, Boston. 83-101.

Hebden, D., Stroud, H.J.F., 1981. Chemistry of coal utilization. New York : John Wiley & Sons Inc. P. 1559-1752.

Hill, T.L. 1996. Adsorption from a one-dimensional lattice gas and the Brunauer-Emmett-Teller equation. Proc. Natl. Acad. Sci. USA 93, 14328-14332.

Hill, G.R., Lyon, L.B., 1962. A new chemical structure for coal. Industrial and engineering chemistry 54, 36-41.

Huggins, F.E., 2002. Overview of analytical methods for inorganic constituents in coal. Int. J. Coal Geol. 50, 169-214.

Huggins, F.E., Kosmack, D.A., Huffman, G.P., 1981. Correlation between ash-fusion temperatures and ternary equilibrium phase diagrams. Fuel 60, 577-584.

Hutchinson, F.H., 2009. About Gasification. [Web:] http://www.clean-energy.us/facts/gasification.htm [Date of use: 11 June 2010].

Innovative Combustion Technologies (ICT), 2006. Slagging and coal-ash quality. [Web:] www.innovativecombustion.com [Date of use: 11 June 2010].

Jenkins, B.M., Bakker, R.R., Wei, J.B., 1996. On the properties of washed straw. Biomass and Bioenergy 10, 177-200.

Kapteijn, F., Abbel, G., Moulijn, J.A., 1984. CO_2 gasification of carbon catalyzed by alkali

metals: Reactivity and mechanism. Fuel 63, 1036-1042.

Kapteijn, F., Peer, O., Moulijn, J.A., 1986. Kinetics of the alkali carbonate catalyzed gasification of carbon. Fuel 66, 1371-1376.

Kotz, J.C., Treichel, P.M., 2003. Chemistry and chemical reactivity. Phoenix : Thomson Brooks/Cole. 997 p.

Kühn, L., Plogmann, H., 1983. Reaction of catalysts with mineral matter during coal gasification. Fuel 62, 205-208.

Lang, R.J., 1986. Anion effects in alkali-catalyzed steam gasification. Fuel 65, 1324-1329.

Larsen, J.W., Green, T.K., Kovac, J., 1989. The nature of the macromolecular network structure of bituminous coals. J. Org. Chem. 50, 4729-4735.

Li, Y., Li, J., Jin, Y., Wu, Y., Gao, J., 2005. Study on alkali-metal vapor removal for high-temperature cleaning of coal gas. Energy and Fuels 19, 1606-1610.

Liu, Y., Gupta, R., Sharma, A., Wall, T., Butcher, A., Miller, G., Gottlieb, P., French, D., 2005. Mineral matter-organic matter association characterization by QEMSCAN and applications in coal utilization. Fuel 84, 1259-1267.

Liu, Y., Gupta, R., Wall, T., 2007. Ash formation from excluded minerals including consideration of mineral-mineral associations. Energy Fuels 21, 461-467.

Liu, Z., Zhu, H., 1986. Steam gasification of coal char using alkali and alkaline-earth metal catalysts. Fuel 65, 1334-1338.

Lloyd, W.G., Riley, J.T., Zhou, S., Risen, M.A., Tibbitts, R.L., 1993. Ash fusion temperature under oxidizing conditions. Energy and Fuels 7, 490-494.

Lucht, L.M., Larson, J.M., Peppas, N.A., 1987. Macromolecular structure of coals. 9. Molecular structure and glass transition temperature. Energy & Fuels 1, 56-58.

Matjie, R.H., Li, Z., Ward, C.R., French, D., 2008. Chemical composition of glass and crystalline phases in coarse coal gasification ash. Fuel 87, 857-869.

Matjie, R.H., French, D., Ward, C.R., Pistorius, P.C., Li, Z. 2011. Behaviour of coal mineral matter in sintering and slagging of ash during the gasification process. Fuel Processing Technology 92, 1426-1433.

Matjie, R.H. 2008. Sintering and slagging of mineral matter in South African coals during the coal gasification process. Doctoral Thesis. Etd-11112008-125913.

McKee, D.W., 1983. Mechanisms of the alkali metal catalyzed gasification of carbon. Fuel 62, 170-175.

McKee, D.W., Spiro, C.L., Kosky, P.G., Lamby, E.J., 1983. Catalysis of coal char gasification by

alkali metal salts. Fuel 62, 217-220.

McLennan A.R., Bryant, G.W., Stanmore, B.R., Wall, T.F., 2000. Ash formation mechanisms during pf combustion in reducing conditions. Energy Fuels 14, 150-159.

Mojtahedi, W., Backman, R., 1989. Release of alkali metals in a pressurized fluidized-bed combustion and gasification of peat. Espoo Technical Research Centre of Finland, Publications 53, 48p.

Moulijn, J.A., Cerfontain, M.B., Kapteijn, F., 1984. Mechanism of the potassium catalyzed gasification of carbon in CO_2. Fuel 63, 1043-1047.

Muchmore, C.B., Hippo, E.J., Chen, H.L., Joslin, J.L., Wang, A., Hughes, A., Sivanandan, S., Daman, E., Banerjee, D.D., 1995. Distribution of sodium, potassium and chlorine between solid and vapor phases under coal gasification conditions. Coal Science 24, 819-822.

Ndaji, F.E., Butterfield, I.M., Thomas, K.M., 1997. Changes in the macromolecular structure of coals with pyrolysis temperature. Fuel 76, 169-177.

Nip, M., De Leeuw, J.W., 1992. Chemical structure of bituminous coal and its constituting maceral fractions as revealed by flash pyrolysis. Energy & Fuels 6, 125-136.

Nishiyama, Y., 1991. Catalytic gasification of coals – Features and possibilities. Fuel Processing Technology 29, 31-42.

Nuffield, E.W., 1966. X-ray diffraction methods. New York : John Wiley and Sons, Inc. 409p.

Olsson, J.G., Jäglid, U., Pettersson, J.B.C., 1997. Alkali metal emission during pyrolysis of biomass. Energy and Fuels 11, 779-784.

Olsson, J.G., Pettersson, J.B.C., 1998. Alkali metal emission from filter ash and fluidized-bed material from PFB gasification of biomass. Energy and Fuels 12, 626-630.

Probstein, R.F., Hicks, R.E., 2006. Synthetic Fuels. New York : Dover Publications. 490 p.

Punjak, W.A., Uberoi, M., Shadman, F., 1989. High-temperature adsorption of alkali vapors on solid sorbents. AIChE Journal 35, 1186-1194

Rietveld, H.M. 1969. A profile refinement method for nuclear and magnetic structure. Journal of applied crystallography 2, 65-71.

Rubiera, F., Arenillas, A., Pevida, C., Garcia, R., Pis, J.J., Steel, K.M., Patrick, J.W., 2002. Coal structure and reactivity changes induced by chemical demineralization. Fuel Processing Technology 79, 273-279.

Sams, D.A., Shadman, F., 1983. Catalytic effect of potassium on the rate of char-CO_2 gasification. Fuel 62, 880-882.

Schobert, H.H. 2008. Coal chemistry. Potchefstroom : North West University. 179 p.

Shadman, F., Sams, D.A., Punjak, A., 1987. Significance of the reduction of alkali carbonates in catalytic carbon gasification. Fuel 66, 1658-1663.

Sheldon, H.D.L., Teats, F.G., Swift, W.M., 1992. Alkali-vapor emission from PFBC of Illinois coals. Combust. Sci. And Tech. 86, 327-336.

Sheth, A., Yeboah, Y.D., Godavarty, A., Xu, Y., Argawal, P.K., 2003. Catalytic gasification of coal using eutectic salts: reaction kinetics with binary and ternary eutectic catalysts. Fuel 82, 305-317.

Shinn, J.H., 1984. From coal to single-stage and two-stage products: A reactive model of coal structure. Fuel 63, 1187-1196.

Silva, I.F., Lobo, L.S., 1986. Study of CO_2 gasification of activated carbon catalyzed by molybdenum oxide and potassium carbonate. Fuel 65, 1400-1403.

Song, W.J., Tang, L.H., Zhu, X.D., Wu, Y.Q., Zhu, Z.B., Koyama, S., 2010. Effect of coal ash composition on ash fusion temperatures. Energy Fuels 24, 182-189.

South African National Standard. SABS ISO 540:2008. Hard coal and coke – Determination of ash fusibility – high temperature tube method. South African Bureau of Standard.

South African National Standard. SABS ISO 562:2010a. Hard coal and coke – determination of volatile matter. South African Bureau of Standard.

South African National Standard. SABS ISO 589:2009. Hard coal – Determination of total moisture. South African Bureau of Standards.

South African National Standard. SABS ISO 1171:2010b. Solid mineral fuels – Determination of ash. South African Bureau of Standard.

South African National Standard. SABS ISO 17025:2006. General requirements for the competence of testing and calibration laboratories. South African Bureau of Standard.

Spiro, C.L., McKee, D.W., Kosky, P.G., Lamby, E.J., 1983a. Catalytic CO_2-gasification of graphite *versus* coal char. Fuel 62, 180-184.

Spiro, C.L., McKee, D.W., Kosky, P.G., Lamby, E.J., Maylotte, D.H., 1983b. Significant parameters in the catalyzed CO_2 gasification of coal chars. Fuel 62, 323-330.

Spiro, C.L., McKee, D.W., Kosky, P.G., Lamby, E.J., 1984. Comparison of effects of adding Boudouard catalysts before and after coal charring. Fuel 63, 133-134.

Spiro, C.L., Wong, J., Lytle, F.W., Greegor, R.B., Maylotte, D.H., Lamson, S.H., 1986. Forms of potassium in coal and its combustion products. Fuel 65, 327-336.

Suzuki, T., Mishima, M., Kitaguchi, J., Itoh, M., Watanabe, Y., 1984. The catalytic steam gasification of one Australian and three Japanese coals using potassium and sodium carbonates. Fuel Processing Technology 8, 205-212.

Suzuki, T., Inoue, K., Watanabe, Y., 1989. Steam pulsed gasification of Na_2CO_3 or $Fe(NO_3)_3$ loaded Yallourn coal char. Fuel 68, 626-630.

Suzuki, T., Ohme, H., Watanabe, Y., 1992. Alkali metal catalyzed CO_2 gasification of carbon. Energy and Fuels 6, 343-351.

Takarada, T., Tamai, Y., Tomita, A., 1986. Effectiveness of K_2CO_3 and Ni as catalysts in steam gasification. Fuel 65, 679-683.

The Physical and Theoretical Chemistry Laboratory Oxford University – Chemical and other safety information. Safety data for potassium carbonate anhydrous. 2011a. [Web:] http://msds.chem.ox.ac.uk/PO/potassium_carbonate_anhydrous.html. [Date of use: 30 Jan. 2011].

The Physical and Theoretical Chemistry Laboratory Oxford University – Chemical and other safety information. Safety data for sodium carbonate anhydrous. 2011b. [Web:] http://msds.chem.ox.ac.uk/SO/sodium_carbonate_anhydrous.html. [Date of use: 30 Jan. 2011].

The South African Coal Processing Society (TSACPS). 2002. Coal Preparation in South Africa. Pietermaritzburg : Natal Witness Commercial Printers. 298 p.

Tran, K., Lisa, M.K., Steenari, B., Lindqvist, O., Hagström, M., Pettersson, J.B.C., 2003. Capture of alkali metals by kaolin. 17th International Fluidized Bed Combustion Conference, Jacksonville. p. 403-409.

Tromp, P.J.J., Karsten, P.J.A., Jenkins, R.G., Mouljin, J.J., 1986. The thermoplasticity of coal and the effect of K_2CO_3 addition in relation to the reactivity of the char in gasification. Fuel 65, 1450-1456.

Tseng, H.P., Edgar, T.F., 1989. The change of the physical properties of coal char during reaction. Fuel 68, 114-119.

Valix, M., Trimm, D.L. 2000. The pore structure development of Australian brown and swelling and non-swelling bituminous coals and its effect on reactivity under regime I and regime II combustion conditions. Adsorption Science and Technology. World Scientific, Singapore, pp. 628-632.

Van Alphen, C., 2007. Automated mineralogical analysis of coal and ash products – challenges and requirements. Miner. Eng. 20, 496-505.

Van Niekerk, D., Pugmire, R.J., Solum, M.S., Painter, P.C., Mathews, J.P., 2008. Structural characterization of vitrinite-rich and inertinite-rich Permian-aged South African bituminous coals. International Journal of Coal Geology 76, 290-300.

Veraa, M.J., Bell, A.T., 1978. Effect of alkali metal catalysts on gasification of coal char. Fuel 57, 194-200.

Veras, C.A.G., Carvalho, J.A., Ferreira, M.A., 2002. The chemical percolation devolatilization model applied to the devolatilization of coal in high intensity acoustic fields. J. Braz. Chem. Soc. 13, 358-367.

Walker, P.L., Hippo, E.J., 1975. Factors affecting reactivity of coal chars. Fuel 54, 245-251.

Walker, P.L., 1981. Microporosity in coal: its characterization and its implications for coal utilization. Phil. Trans. R. Soc. Lond. A 300, 65-81.

Wall, T.F., Creelman, R.A., Gupta, R.P., Gupta, S.K., Coin, C., Lowe, A., 1998. Coal ash fusion temperatures – new characterization technique, and implications for slagging and fouling. Prog. Energy. Combust. Sci. 24, 345-353.

Wall, T.F., Gupta, S.K., Gupta, R.P., Sanders, R.H., Creelman, R.A., Bryant, G.W., 1999. False deformation temperatures for ash fusibility associated with the conditions for ash preparation. Fuel 78, 1057-1063.

Ward, C.R., 2002. Analysis and significance of mineral matter in coal seams. Int. J. Coal Geol. 50, 135-168.

Ward, C.R., French, D. 2004. Analysis and significance of mineral matter in coal, The society for organic petrology. Short course notes, The University of New South Wales, Sydney, NSW, Australia. p. 7-68.

Weeber, S., Cairncross, B., Falcon, R.M.S., 2000. Mineralogical, petrographic and geological controls on coal ash fusion temperature from New Clydesdale Colliery, Witbank Coalfield, South Africa. The Journal of the South African Institute of Mining and Metallurgy 3, 181-190.

Westberg, H.M., Byström, M., Leckner, B., 2003. Distribution of potassium, chlorine, and sulfur between solid and vapor phases during combustion of wood chips and coal. Energy and Fuels 17, 18-28.

Witthohn, A., Oeltjen, L., Hilpert, K., 1998. Release and sorption of alkali metals in coal conversion. Proceedings of the International Joint Power Generation Conference, Germany 1, 161-168.

Wood, B.J., Fleming, R.H., Wise, H., 1984. Reactive intermediate in the alkali-carbonate-

catalyzed gasification of coal char. Fuel 63, 1600-1603.

Wood, L.J., Breithaupt, L.J. 1952. Reaction between dry inorganic salts. Viii. Refractive Index study of solid solutions formed by the reciprocal system RbCl + KBr = RbBr + KCl, May 5.

Zhang, J., Han, C., Yan, Z., Liu, K., Xu, Y., Sheng, C., 2001. The varying characterization of alkali metals (Na, K) from coal during the initial stage of coal combustion. Energy and Fuels 15, 786-793.

Zhao, B., Zhang, Z., Wu, X., 2010. Prediction of coal ash fusion temperature by least-squares support vector machine model. Energy Fuels 24, 3066-3071.

Zhu, W., Song, W., Lin, W., 2008. Catalytic gasification of char form co-pyrolysis of coal and biomass. Fuel Processing Technology 89, 890-896.